Modelling and Control of Epidemics Across Scales

Esteban A. Hernandez-Vargas [a], Alejandro H. González [b], Carolyn L. Beck [c], Xiaoqi Bi [c], Francesca Calà Campana [d], Giulia Giordano [d]

***Abstract*— When facing the global health threat posed by an infectious disease, predictive mathematical models are crucial not only to understand and forecast the epidemic evolution, but also to plan effective control strategies that contrast the disease and its spread in the population. This tutorial aims to give a broad overview of the fundamental developments enabled by systems-and-control methodologies in modelling and controlling epidemiological dynamics across scales, from infection dynamics within hosts to contagion dynamics between hosts. The first part is focused on modelling and control of infectious diseases in the host, capturing the dynamic interplay between pathogens and the immune system, and discussing control strategies to design tailored therapies and treatments to optimally clear the infection. The second part deals with the spread of contagion between hosts: epidemic dynamics are modelled resorting to networked systems where the nodes represent individuals and the links represent interactions that can lead to contagion, and a comparison to compartmental models is carried out. The third part surveys multi-scale models and multi-pronged approaches to contrast the spread of infectious diseases: a holistic perspective is adopted, including behavioural and socio-economic aspects along with public health issues, to discuss optimal epidemic control across scales.**

I. Introduction

Infectious diseases are a global health threat: the world has recently faced outbreaks of Ebola, SARS, MERS, tropical diseases, monkeypox, and the HIV and COVID-19 pandemics. Mathematical models are crucial to monitor, predict, prevent and control epidemics. This tutorial surveys the fundamental developments in modelling and controlling infectious diseases, seen as complex phenomena that embrace multiple scales, from the microscopic scale of infection dynamics within a host (the interplay between pathogens and immune system at the individual level) to the macroscopic scale of contagion between hosts (the epidemic spreading of the disease between individuals at the population level).
The three tutorial contributions focus on diverse aspects to offer a well-rounded illustration of control-theoretic methods to model and control infectious diseases across scales.

Mathematical models of viral spread processes have been analysed for over 200 years, with one of the earliest treatments presented by Bernoulli in his pioneering work on smallpox infection dynamics [1]. In [2], [3], Kermack and McKendrick laid the foundations for mean-field *compartmental models*, still widely used today [4]–[8]. These models assume that every subject, or agent, lies in a single compartment, or subgroup, of a well-mixed population at any given time; the compartments are associated with different stages of the disease and can include *susceptible*, *exposed*, *asymptomatic (infected)*, *(symptomatic) infected*, *recovered*, and/or *immunised* population groups, as well as *vaccinated*, *quarantined*, *hospitalised*. Classic epidemiological models are the SIS (susceptible-infected-susceptible) and SIR (susceptible-infected-recovered) models, with renewed interest in SEIR (susceptible-exposed-infected-recovered) and SAIR (susceptible-asymptomatic-infected-recovered) models due to COVID-19 [9]–[13]. More detailed compartmental models capture specific infectious disease dynamics, including e.g. the effect of non-pharmaceutical interventions (NPIs), such as physical distancing, testing and contact tracing [14], [15], and of mass vaccination [16]. The SIDARTHE model [15], [16] emphasises the role of asymptomatic transmission, which often eludes diagnosis, and the different severity of symptoms in different individuals, potentially leading to hospitalisation, intensive care unit (ICU) admission, or death.

While compartmental models assume that the agents in the population are well-mixed, a large and growing body of work considers the spread of epidemics over complex and realistic network structures that capture the actual contact patterns in society [17]–[20]. Understanding how dynamical contagion processes evolve across different network structures (the rates at which they spread as a function of network structure, and how multiple viral types and multiple network layers affect the spread process dynamics) leads to a greater understanding as to how to contain and mitigate future viral outbreaks.

To combat an infectious disease, it is also fundamental to treat the infection in each host: mechanistic models of the interplay between the disease and the immune system [21]–[26], and the available drugs, need to be developed to design optimal therapies that mitigate the infection with

[a] Department of Mathematics and Statistical Science, University of Idaho, Moscow, Idaho, 83844-1103, USA. esteban@uidaho.edu

[b] Instituto de Desarrollo Tecnológico para la Industria Química (INTEC), Consejo Nacional de Investigaciones científicas y tecnicas (CONICET) and Universidad Nacional del Litoral (UNL), Santa Fe, Argentina. alejgon@santafe-conicet.gov.ar

[c] Department of Industrial and Enterprise Systems Engineering, University of Illinois at Urbana-Champaign, USA. {beck3,xiaoqib2}@illinois.edu

[d] Department of Industrial Engineering, University of Trento, Italy. {f.calacampana,giulia.giordano}@unitn.it

Esteban Hernandez-Vargas was supported by the National Institute Of General Medical Sciences of the National Institutes of Health under Award Number P20GM104420. The content is solely the responsibility of the authors and does not necessarily represent the official views of the NIH.

Carolyn L. Beck and Xiaoqi Bi acknowledge the support of: the C3.ai Digital Transformation Institute sponsored by C3.ai Inc. and the Microsoft Corporation; the Jump ARCHES endowment through the Health Care Engineering Systems Center of the University of Illinois at Urbana-Champaign; and the National Science Foundation NSF-ECCS 2032321.

Francesca Calà Campana and Giulia Giordano acknowledge the support of the Strategic Grant MOSES at the University of Trento.

the smallest possible side effects. The optimal planning of antiviral treatments for HIV [27]–[29] (and, similarly, of cancer therapies [30]–[32]) have been recently addressed.

Control of infectious diseases is a multidisciplinary field linking the application of engineering principles, mathematical modelling, medicine, and biology to address healthcare challenges. Models are crucial to (i) unveil the mechanisms of epidemic phenomena at all scales, from in-host infection dynamics to between-host contagion dynamics, (ii) forecast their evolution with parameters estimated based on the available data [33], and (iii) plan optimal therapies to mitigate the infection in the individual host [27], and devise optimal control strategies [34]–[50] to curb the contagion between hosts, resorting to multi-pronged interventions [51]–[53] that are both pharmaceutical (drugs and vaccines) and non-pharmaceutical (use of personal protective equipment, physical distancing, travel bans, lockdown) [42], [54]–[60].

Public measures, essential to contain the contagion, need to be carefully planned to maximise their effectiveness and account for opinion-driven adherence to guidelines, treatments and vaccination. The interplay between contagion and opinion-driven behaviours can be captured by coupling epidemic dynamics with opinion dynamics describing how the attitude towards responsible behaviour evolves in the population, driven by the individual perception of danger, thus affecting the spread of the infection [61]–[66].

A. Modelling and Control of Infectious Diseases in the Host

The contribution by Esteban A. Hernandez-Vargas and Alejandro H. González aims to present interdisciplinary tools to tackle infectious diseases at the host level. Detailed contributions of key players of the immune system to infectious diseases as well as their respective interactions will be discussed. Parameter fitting procedures to adjust parameters based on experimental data will be developed. Consequently, mathematical models will serve to perform stability analysis and control strategies for personalized therapies based on in-hosts models for several viral infections. Concepts as the critical fraction of susceptible/non-infected cells (under which the infection can no longer increase) can be fully understood and used in more general control objectives if put in terms of the equilibrium sets and their stability. Based on classical Lyapunov methods, a full characterization of the dynamical behaviour of the target-cell models under control actions will be discussed. Furthermore, based on the concept of virus spreadability, antiviral effectiveness thresholds are determined to establish whether a given treatment will be able to clear the infection. Also, it is shown how to simultaneously minimize the total fraction of infected cells while maintaining the virus load under a given level. Parameter fitting, modelling, and control applications are discussed.

B. Epidemic Process Dynamics over Networks

The contribution by Carolyn L. Beck and Xiaoqi Bi discusses a family of mathematical models that have been proposed to capture the dynamic behavior of epidemic processes over networks, allowing for an agent-based perspective of spread process dynamics. Networked epidemic models are introduced and compared to traditional compartmental epidemiological models, focusing on stability analyses for examples from both model types. Compartmental epidemiological models assume that the agents in the population are well-mixed, implying that the underlying contact network between the subjects is a complete graph. Over the past two decades, there has been a broad study of epidemic processes over more complex and more realistic network structures than complete graph structures [18]–[20], [67]. To account for network structure among individuals or subgroups of a population, an agent-based perspective is used, where we assume each agent is represented by a node in the network, and the edges between the nodes represent the strength of the interaction between agents. Agents, or nodes, may represent either individuals or subgroups in the population.

Assuming a total of n agents in a population model, spread processes can be described in a probabilistic framework by large Markov process models that provide the probability of each agent transitioning from one disease state to another, for example from susceptible to infected, and/or to recovered states, and back. These probabilities are determined by the infection, healing and/or recovery rates, in addition to the underlying network graph structure, and model the stochastic evolution of such processes. For SIS processes, these Markov process models will have dimension 2^n, and dimension 3^n for SIRS models. As a result these models are difficult, if not intractable, to analyze, thus it is typically assumed the number of agents is large enough that *mean-field approximations* (MFAs) are valid, derived by taking expectations over the infection transition rates of the agents, followed by evaluation of the limiting behavior of the expectation dynamics as the time interval of interest decreases to zero [68]. For agents interconnected via a graph with a weighted adjacency matrix, the use of MFA models to describe the dynamical behavior of an epidemic process over a network is now largely accepted under the assumption that the population size is large and relatively constant, along with additional independence assumptions, and can provide upper bounds on probabilities of infection for the agents at any given time [68], [69]. Network-dependent ordinary-differential-equation (ODE) continuous-time SIS models have been studied extensively [18], [68], [70] and [71] also considers time-varying networks. Discrete time versions of MFA models are in [72]–[74].

Most stability studies of epidemic process dynamics analyze the system equilibria and determine the convergence behavior of these processes near isolated equilibria, specifically searching conditions for the existence of and convergence to either the *disease-free* (healthy state) or a *non-disease-free* (endemic state) equilibrium. For the networked SIS model, for example, when the condition for the disease-free equilibrium (DFE), which depends on the parameters of the model, does not hold, then there exists another equilibrium, i.e., an endemic equilibrium, that is (almost) globally asymptotically stable [73], [75]–[78]. Similar differential equation-based models for SIR processes have also been studied; an analysis of equilibria and convergence properties for static-

network SIR models is given in [17]. Exact Markovian process dynamics for SIR epidemics are discussed in [79].

C. Multi-Pronged Interventions to Contrast Epidemics

The contribution by Francesca Calà Campana and Giulia Giordano presents a holistic viewpoint on epidemics that spans across multiple scales and includes opinion dynamics and socio-economic aspects along with public health issues.

Control theory provides a convenient mathematical framework to plan interventions that contain the contagion [18]. Mathematical tools such as bifurcation theory and Lyapunov theory can characterise the different possible qualitative behaviours of epidemic phenomena and determine the role played by the various model parameters in the spread of contagion. Hence, a suitable manipulation of these parameters allows to control the dynamics. Several measures to contrast epidemics are discussed in the literature; see [33] and the references therein for a recent survey. NPIs are often the only available strategy to contrast new pathogens, for which no drugs or vaccines yet exist. However, physical distancing and lockdown have relevant social and economic costs; hence, they should be adopted at carefully chosen moments [80], with a pre-emptive approach [81], and for limited time periods [82]. On the other hand, pro-active testing and contact-tracing [83] need to cope with the limited availability of reagents and testing infrastructures. In the presence of constraints, trade-offs, and possibly conflicting multi-objective goals, optimal control theory [34]–[50] suggests approaches to reduce the burden of an epidemic by determining the optimal allocation of limited resources (e.g. reagents or vaccines), or the optimal implementation of NPIs.

Yet, the countermeasures are not always adopted widely by the population. Adherence to restrictions and vaccination campaigns is driven by the individual opinions that determine the actual behaviours, which in turn affect the spread of contagion. To capture such intertwined dynamics, behavioural epidemiology [61]–[66] couples human behaviour with the transmission and control of an infectious disease: the information on the spread of the disease, obtained e.g. via mass media or social networks, is summarised by the information index (a concept that extends the modelling approach in [84], which captures the behavioural response of individuals to the prevalence of the disease), and influences individual behaviours and willingness to vaccinate.

Finally, an all-encompassing perspective is offered by interdisciplinary multi-scale epidemic models that integrate epidemiology, immunology, economy, sociology and mathematics [85]. Holistic multi-scale models [86]–[96] capture both in-host infection dynamics, at the individual level, and between-host contagion dynamics, at the population level, thus considering the mutual interplay between immunological and epidemiological phenomena. The enormous complexity of these models and the scarcity of suitable datasets [96]–[98] pose noteworthy challenges to the systematic implementation of multi-scale models. However, the simultaneous understanding of infection and contagion dynamics, as well as of their coupling, is crucial to enable the rigorous design of mathematical control approaches for effective disease suppression, or mitigation, across scales.

II. Modelling and Control of Viral Infections in the Host

A. Modelling In-Host Infections

Mathematical models of infectious diseases have been developed at different scales [99]. While between-hosts models are central to support public health strategies [15], within-host models are important to capture the dynamics of different pathogens and their respective interactions with the immune system. Furthermore, control theoretical tools can serve to schedule therapies [100], [101].

In this tutorial, we will introduce how mathematical modelling and control theory can serve to evaluate dose-response and predict the effect-time courses resulting from specific treatment. We will give a very brief introduction to the immune system and the most used mathematical models to represent in-host infections.

The immune system can be divided into innate and adaptive. When a pathogen, such as a virus or bacterium, is recognized by the innate immune system, fast and non-specific mechanisms take place to clear the pathogen. Then, the adaptive immune responses are tailored to clear specifically the pathogen or infected cells. Further reference for immunology can be found in [102]. To avoid harming the host, the immune system has regulatory mechanisms to regulate itself. Fig.1 illustrates the basic connections between the immune system to clear a pathogen in the host.

Mechanistic models can help us to mimic infectious diseases and their respective biological mechanisms. Models can be either pedagogical tools to understand and predict disease progression or objects of further experiments. Model selection is a central part of modelling that can be performed by fitting the models to experimental data and comparing the models' goodness-of-fit criterion.

To perform parameter fitting using experimental data and models based on ordinary differential equations or partial differential equations, the reader can use the python module *PDEparams* [103]. This can provide a flexible interface for different parameter analysis such as computation of likelihood profiles [104], parametric bootstrapping and confidence intervals [105], along with direct visualization of the results.

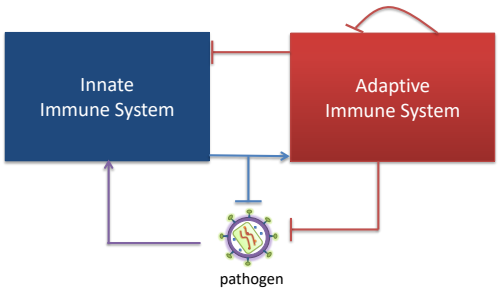

Fig. 1: Immune System Components. Pointed arrows represent activation, while hammer-headed arrows represents inhibition.

How to formulate mechanistic models for infectious diseases in the host? Experimental data enable mathematical modeling, model parameters are estimated for model candidates using experimental data, along with mathematical and biological concepts depending on the model application [106], and parameter uncertainty is dealt with in order to enable robust model predictions that can then be compared with experimental data. However, multiple model structures can give the same fit for a given data set. Thus, a model selection criterion such as the Akaike Information Criterion (AIC) [107] can be used to select, based on the complexity, the model that has the best fit for the data. Parameter uncertainty is evaluated by parameter confidence intervals and sensitivity analysis. This is relevant to show the relation between parameters and their respective influence on the model outcome. Once model parameter distributions are inferred, models can be tested towards new knowledge of the observed process and guiding the design of new experiments.

B. Target-Cell-Limited Model for In-Host Acute Infection

The most used mathematical model to represent viral dynamics in the host is the target cell-limited model. While simple in its structure, the target cell-limited model has served to describe several viral diseases [108], among which are HIV [109], hepatitis [110], influenza [111], ebola [112], zika [113], and SARS-CoV-2 [114], [115]. A detailed reference for modelling of viral dynamics can be found in [116]. The following ordinary differential equations (ODEs) describe the target cell model:

$$\dot{U}(t) = -\beta(t)U(t)V(t), \qquad U(0) = U_0, \tag{1a}$$

$$\dot{I}(t) = \beta(t)U(t)V(t) - \delta I(t), \qquad I(0) = I_0, \tag{1b}$$

$$\dot{V}(t) = pI(t) - cV(t), \qquad V(0) = V_0, \tag{1c}$$

where the state variables are uninfected target or susceptible cells $U(t)$ [cell/mm^3], infected cells $I(t)$ [cell/mm^3], and virus $V(t)$ [copies/mL], at time t. The parameter $\beta(\cdot)$ [mL.day^{-1}/copies] is the infection rate of healthy U cells by external virus V, δ [day^{-1}] is the death rates of I, p [(copies.mm^3/cell.mL).day^{-1}] is the viral replication, and c [day^{-1}] is degradation (or clearance) rate of the virus V. A numerical example of the target cell-limited model is shown in Fig. 2. An exponential growth takes places in infected cells and viral load; then, due to the limited amount of target cells, infected cells and viral load decrease.

Remark 1: The immune system is not explicitly represented in model (1). However, the parameters δ and c are adjusted to clinical data, which can be considered an indirect representation of the immune system to clear infected cells and fast the viral clearance.

System (1) is positive under positive initial conditions. We denote $x(t) := (U(t), I(t), V(t))$ the state vector and $\mathcal{X} = \mathbb{R}^3_{\geq 0}$ the state constraints set. The infection time is $t = 0$, i.e., $V(0) = V_0$, $I(0) = I_0 = 0$ and $U(0) = U_0$, where V_0 is a small amount of virus at $t = 0$. $U_0 > 0$ represents the total number of susceptible cells in a healthy state.

Remark 2: The infection rate β is in general time-varying, since this parameter is affected by the immune system and antiviral treatments (control actions). While the antivirals do not eliminate directly the virus, they can inhibit the replication cycle; that is, parameters β and p are reduced. Both parameters affect the reproduction number (defined next) in the same way [117].

To account for the effect of the immune system or antiviral treatments, it is assumed that $\beta(\cdot) \in \Omega_\beta$, where Ω_β is the set of functions $\beta(\cdot) : \mathbb{R}_{\geq 0} \to \mathbb{R}_{>0}$ such that $\beta(t) \in [\underline{\beta}, \overline{\beta}]$, for $t \in [t_i, t_f]$, and $\beta(t) = \overline{\beta}$, for $t \in [0, t_i) \cup (t_f, \infty]$, being $0 < t_i < t_f < \infty$ the starting and ending treatment time. t_f is assumed to be finite since acute infection treatments are always finite-duration treatments. $0 < \underline{\beta} < \overline{\beta}$ are the minimal and maximal values of the infection rate, respectively. $\underline{\beta}$ and $\overline{\beta}$ represent the untreated and fully treated infection rate, respectively; the case $\underline{\beta} = 0$ is not considered since antivirals have a limited effect on the infection rate. Fig.3 shows an illustration of $\beta(t)$ representing the potential effect of the immune system and antivirals.

Although the solution of (1) for $t \geq 0$ is unknown (even for a fixed β), we can make some simple analysis to gain some insight into the general system behavior. According to [117], if c is much larger than δ, system (1) can be approximated by $\dot{U}(t) \approx -\beta(t)U(t)V(t)$, $\dot{V}(t) \approx (\frac{\beta(t)p}{c}U(t) - \delta)V(t)$, $I(t) = \frac{c}{p}V(t)$. Then, since $U(t) > 0$ for all $t \geq 0$, conditions for $\dot{V}$ to decrease at some $t > 0$ are given by $U(t) < \frac{c\delta}{\beta(t)p}$. Furthermore, $U_0 = U(0) > \frac{c\delta}{\beta(0)p} = \frac{c\delta}{\overline{\beta}p}$ (since otherwise there is no an infection) and, according to (1.a) $U(t)$ is decreasing for all $t \geq 0$. Then, since $\beta(t) \leq \overline{\beta}$ for all $t \geq 0$, once $U(t)$ crosses $\frac{c\delta}{\overline{\beta}p}$ from above, it cannot longer be greater than $\frac{c\delta}{\beta(t)p}$ (i.e., $\frac{c\delta}{\beta(t)p} \geq \frac{c\delta}{\overline{\beta}p}$ for all $t \geq 0$), and V cannot longer grow (once $U(t) < \frac{c\delta}{\overline{\beta}p}$ it can be considered that the virus would no longer spread in the host ([117]), since there is no future time instants for which $\dot{V} > 0$). This threshold value for U is denoted as the critical susceptible cells threshold

$$U^* := \frac{c\delta}{\overline{\beta}p}, \tag{2}$$

and it can be seen as the counterpart of the 'herd immunity' in the epidemiological SIR-type models [118].

1) Equilibria and Stability: A control equilibrium is, by definition, an equilibrium of the system (1) associated to any

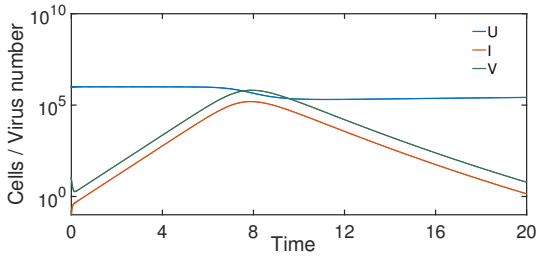

Fig. 2: Target cell limited model simulation. Model initial conditions $U(0) = 10^6$, $I(0) = 0$, and $V(0) = 10$ were considered. Model parameters $d_u = 0.01$, $\beta = 10^{-7}$, $\delta = 2$, $p = 100$, and $c = 24$ were assumed.

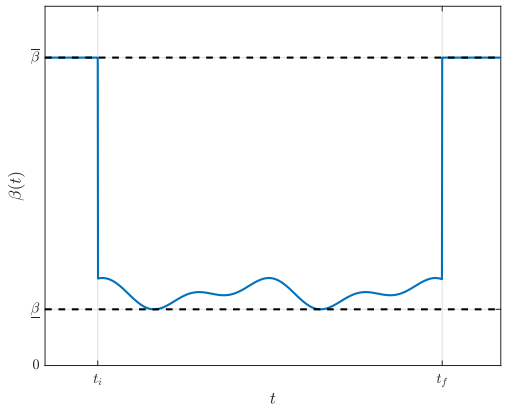

Fig. 3: General form of $\beta(\cdot) \in \Omega_\beta$.

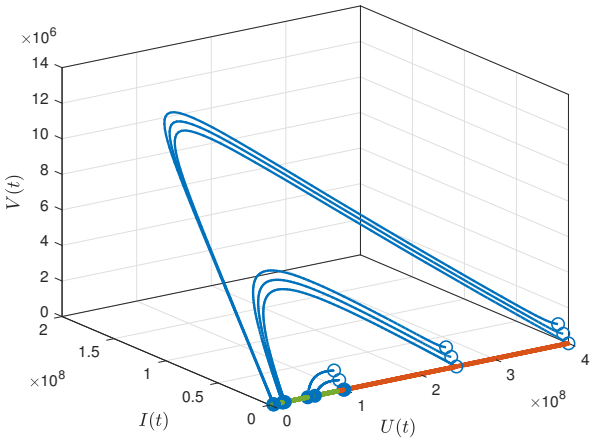

Fig. 4: Phase portrait for a virtual patient, with $U(t_f) > U^*$. States $x(t_f)$, denoted as empty circles, that are arbitrarily close to $\mathcal{X}_s^{un}$ (in red), converge to $\mathcal{X}_s^{st}$ (in green), so the virus spreads in the host. Filled circles represent states for $t \to \infty$.

control action $\beta(\cdot) \in \Omega_\beta$. However, in our case, the control action is a finite-duration signal, so equilibria (i.e., states at which the system can remain indefinitely) can only be considered for $t \geq t_f$, where $\beta(t) = \overline{\beta}$ (because of the form of $\beta(\cdot) \in \Omega_\beta$, the system behavior before t_f is, by definition, at a transient regime). This is equivalent to defining the open-loop equilibrium of (1) with $\beta(t) = \overline{\beta}$ that, by zeroing the differential equations, is given by:

$$\mathcal{X}_s := \{(U, I, V) \in \mathcal{X} : \ U \in [0, U_0], \ I = 0, \ V = 0\}. \quad (3)$$

This set can be divided into two subsets: $\mathcal{X}_s^{st} := \{(U, I, V) \in \mathcal{X} : U \in [0, U^*], \ I = 0, \ V = 0\}$ and $\mathcal{X}_s^{un} := \{(U, I, V) \in \mathcal{X} : U \in (U^*, U_0], \ I = 0, \ V = 0\}$, which allows us to state the following fundamental Theorem of stability:

Theorem 1: Consider the system (1) constrained by $\mathcal{X}$, with $\beta(\cdot) \in \Omega_\beta$. Then, the set $\mathcal{X}_s^{st}$ is the unique asymptotically stable equilibrium set (i.e., the smallest attractive and the largest locally $\epsilon - \delta$ stable set), with a domain of attraction (DOA) given by $\mathcal{X} \backslash \mathcal{X}_s^{un}$, while $\mathcal{X}_s^{un}$ is unstable.

Proof: See [115]. ■

Fig. 4 shows phase portrait plots of the system (1), corresponding to different states $x(t_f)$, for $t > t_f$.

2) Infection final size and viral load peak: Stationary vs transient behavior: The fact that t_f is finite and $\beta(t) = \overline{\beta}$ for $t > t_f$ allows us to state some basic final conditions for the system (1). By defining $U_\infty := \lim_{t\to\infty} U(t)$, $V_\infty := \lim_{t\to\infty} V(t)$ and $I_\infty := \lim_{t\to\infty} I(t)$, we know that $V_\infty = I_\infty = 0$ while U_∞ is given by:

$$U_\infty := -U^* W(-\frac{U(t_f)}{U^*} e^{-\frac{1}{U^*}(U(t_f)+I(t_f)+\frac{\delta}{p}V(t_f))}), \quad (4)$$

where $W(\cdot)$ is the Lambert function (see [117] for details). This way, U_∞ is an explicit function of the system parameters $(\overline{\beta}, \delta, p, c)$ and the states at t_f, $x(t_f) = (U(t_f), I(t_f), V(t_f))$, but not of $\beta(\cdot)$ (i.e., $\beta(t)$ affect U_∞ only trough $x(t_f)$).

According to well-known results (see [119], for the case of SARS-CoV-2) the two main indexes describing the severity and infectiousness of the disease are the infection final size (IFS), which indicates the amount of infected (dead) cells at the end of the infection an so the probability for the host to develop co-infections and related side effects, and the viral load peak (VLP), which indicates both, the severity of the disease and also the infectiousness of the host (ability to transmit the virus to other hosts). These two indexes are defined as:

$$IFS := U_0 - U_\infty, \quad (5)$$

$$VLP := \max_{t\in[0,\infty)} V(t), \quad (6)$$

and the objective of a potential control strategy (i.e., limited antiviral treatment schedules that reduce as long as possible the side effects) is to reduce as long as possible these two indexes.

The following Lemma, which establishes conditions to minimize the IFS and the area under the curve of the viral load $AUC_{VL} := \int_0^\infty V(\tau)d\tau$ (which is related to the VLP) for any $\beta(\cdot) \in \Omega_\beta$, sheds some light on the control problem.

Lemma 1: Consider the system (1) constrained by the positive set $\mathcal{X}$, with $\beta(\cdot) \in \Omega_\beta$. Then, the only way to minimize IFS and AUC_{VL} is by implementing a control $\beta(t)$ such that $(U(t_f), I(t_f), V(t_f)) \approx (U^*, 0, 0)$ (i.e., the system approaches the steady state corresponding to $U = U^*$, at t_f). Furthermore, the infimum for the IFS and the AUC_{VL} are given by $IFS^{min} = U_0 - U^*$ and $AUC_{VL}^{min} = \frac{p}{c\delta}(U_0 - U^*)$, respectively.

Lemma 1 is a strong result concerning any kind of control action $\beta(\cdot) \in \Omega_\beta$. It says that there is only one way to arbitrarily approach the unique infimum of the IFS and AUC_{VL} and this depends on the state at the end of the treatment, $x(t_f)$, not on the form of $\beta(t)$. This means that among all the possible $\beta(\cdot) \in \Omega_\beta$ fulfilling the condition $(U(t_f), I(t_f), V(t_f)) \approx (U^*, 0, 0)$, one can select the one that maintains the VLP under a given upper bound (established according the disease severity and host infectiousness), since only the integral of V is fixed (i.e.,

$AUC_{VL} = AUC_{VL}^{min}$) but not its peak.

From a pure dynamic point of view, one can say that minimizing the IFS and the AUC_{VL} is independent of keeping the VLP arbitrary low. Even more, minimizing the IFS and AUC_{VL} is a stationary objective, while keeping VLP arbitrary low is a transient one.

C. Control Strategies to Tailor Antiviral Therapies

The following definition formalizes the control objectives of the problem under study:

Definition 1 (Control objectives): The control objective for the closed-loop (1) consists in (i) minimizing the IFS, and (ii) keeping the VLP under a given upper bound V_{max} (determined by the severity of the disease and the host infectiousness), while minimizing, as long as possible, the total amount of administered antiviral (to avoid drug side effects).

Thus, the control problem consists in finding a function $\beta(\cdot) \in \Omega_\beta$ accounting for the control objective in Definition 1. In view of the dynamic analysis made in the previous sections, we can pose the following optimal control problem $\mathcal{P}_{opt}(U(0), I(0), V(0), U^*, V_{max}; \beta(\cdot))$ that, in contrast to many other strategies, take advantage of the stationary/transient distinction for each of the objectives:

$$\min_{\beta(\cdot)} \quad J(\beta(\cdot)) = \int_0^T [\overline{\beta} - \beta(t)]dt$$

subject to the system (1) and:

$$(U(t), I(t), V(t)) \in \mathcal{X}, \; V(t) \leq V_{max}, \quad t \in [0, T],$$
$$U(T) = U^*, \quad V(T) \leq V_{det}, \quad \beta(\cdot) \in \Omega_\beta,$$

where $T > t_f$ is a large enough time that covers the whole dynamic of the infection. Conditions $V(t) \leq V_{max}$ forces variable $V(\tau)$ to be smaller than the externally imposed maximum V_{max} at every time $t \in [0, T]$, while constraints and $U(T) = U^*$ and $V(T) \leq V_{det}$, where V_{det} is a small detectable virus variable (usually 100 [copies/mL]), force variable $U(t)$ to be equal to U^* at the end time T, at a quasi steady state condition (i.e., with $V(T)$ approaching zero). The key point of Problem $\mathcal{P}_{opt}$ is that the clinical objectives (i.e., controlling the IFS and the VLP) are imposed by constraints while only the objective of minimizing the antiviral is achieved by optimality, so the competition between them is avoided.

Remark 3: It can be shown that Problem $\mathcal{P}_{opt}$ is well-posed and properly accounts for the control objectives in Definition 1. Furthermore, any other optimization problem, i.e., the one minimizing $V(t)$ (or $U(t) = U^*$) along T, without terminal constraints, will necessarily produce a suboptimal solution, since this way the control objectives compete one to each other in the cost function.

1) Numerical Simulations: Here we simulate a virtual patient, denoted as patient A, whose parameters were estimated in [114], [119]. Figure 5 (upper panel, dashed blue and red lines), shows the open-loop system time evolution, which consists in using $\beta(t) \equiv \overline{\beta}$ (no treatment is a particular case of $\beta(\cdot) \in \Omega_\beta$), while Figure 5 (lower panel, dashed blue lines) shows the phase portrait in the plane U, V. As

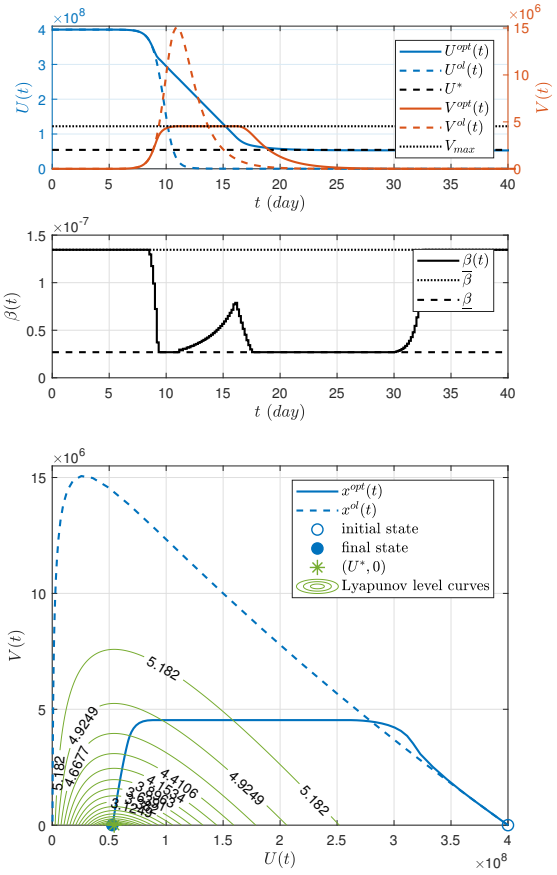

Fig. 5: U (blue), V (red) and β (black) time evolution (left), and phase portrait (upper panel, blue), corresponding to open loop (dashed line) and optimal control (solid line). The model parameters are given by $\overline{\beta} = 1.35 \times 10^{-7}$, $\delta = 0.61$, $p = 0.2$ and $c = 2.4$. The initial conditions are given by: $U_0 = 4 \times 10^8$ [cell/mm^3], $I_0 = 0$ [cell/mm^3] and $V_0 = 0.31$ [copies/mL]. Furthermore, the critical value for the susceptible cells is $U^* = 5.44 \times 10^7$ [cell/mm^3] and $V_{max} = 4.5326 \times 10^6$ [copies/mL].

predicted, U_∞^{ol} is (significantly) smaller than U^* ($IFS^{ol} = U_0 - U_\infty^{ol} = 3.9974 \times 10^8$ [cell/mm^3]), while the peak of V is given by $VLP^{ol} = 1.5064 \times 10^7$ [copies/mL] (the viral load is considered undetectable under the detectable value of $V_{det} = 100$ [copies/mL]).

Figure 5 (lower panel, solid blue and red lines) shows also the optimal control system time evolution, considering a $\beta(t)$ (left, solid black lines) obtained from P_{opt}. The time horizon T was selected to be 32.8 [days] while the maximal allowed VLP is given by $V_{max} = 4.5326 \times 10^6$ (30 % of VLP^{ol}). As it can be seen, the control objectives are reasonably approached, with $IFS^{opt} = 3.4723 \times 10^8$ [cell/mm^3] (80 % of IFS^{ol}), $VLP^{opt} = V_{max} = 4.5326 \times 10^6$ [copies/mL], while the total amount of antiviral is minimized.

Note that $\beta(\cdot)$ separates the control objectives over time: first, it handles the VLP (from $t \approx 8$ to $t \approx 17$ days) and, once V cannot further increase, it tries to reach $U(T) \approx U^*$, at steady-state, to minimize IFS. Although not simulated here, it can be shown that any other optimization problem, for instance the one minimizing the viral load along the time (as

it is usually done in the literature), systematically produces a suboptimal performance, avoiding the achievement of the control objectives.

Remark 4: A better description of the control would be considering the system (1) with the pharmacokinetic and pharmacodynamic of a particular antiviral, which includes also the impulsive nature of the doses (pill intakes) that affect parameter β and p, as it is shown in [115] for the case of SARS-CoV-2. However, the optimality concepts introduced in this tutorial are not altered.

III. Modelling and Analysis of Epidemics over Networks: An Overview

We discuss the modelling, analysis and estimation of epidemic dynamics for a selection of traditional compartment models, and networked models. After providing an overview of classic epidemiological compartment models, we present their networked versions that explicitly account for underlying human contact, transportation, and/or community interaction networks that affect the transmission of epidemic processes, focusing on the SIS and SAIR models. Then we discuss stability and convergence analysis results for some compartmental as well as networked epidemic process models, highlighting the main differences.

1) Notation and Background: Given two vectors $x_1, x_2 \in \mathbb{R}^n$, $x_1 \geq x_2$ indicates each element of x_1 is greater than or equal to the corresponding element of x_2, $x_1 > x_2$ indicates each element of x_1 is greater than or equal to the corresponding element of x_2 and $x_1 \neq x_2$, and $x_1 \gg x_2$ indicates that each element of x_1 is strictly greater than the corresponding element of x_2. Given a matrix $M \in \mathbb{R}^{n\times n}$, the spectral radius of M is $\rho(M)$. Also, m_{ij} indicates the i,j^{th} entry of M. The notation $\mathrm{diag}(\cdot)$ refers to a diagonal matrix with the argument on the diagonal; $[n]$ refers to the set $\{1,\dots,n\}$. The identity matrix is denoted by I, the all-ones vector by $\mathbf{1}$, and the all-zeros vector by $\mathbf{0}$; we assume I, $\mathbf{1}$, and $\mathbf{0}$ have the appropriate dimensions whenever used. $E[\cdot]$ denotes the expected value of the argument and $Pr[\cdot]$ the probability of the argument.

A matrix $X \in \mathbb{R}^{n\times n}$ is *reducible* if there exists a permutation matrix T such that $T^{-1}XT = \begin{pmatrix} Y & Z \\ 0 & W \end{pmatrix}$, where Y and W are square matrices, or if $n = 1$ and $X = 0$. A real square matrix is called irreducible if it is not reducible.

Network structures and graphs: A *directed graph*, or *digraph*, is a pair $\mathcal{G} = (\mathcal{V}, \mathcal{E})$, with set of nodes $\mathcal{V}$ and set of edges $\mathcal{E} \subseteq \mathcal{V} \times \mathcal{V}$. Given $\mathcal{G}$, we denote an edge from node $i \in \mathcal{V}$ to node $j \in \mathcal{V}$ by (i,j). Node $i \in \mathcal{V}$ is a neighbor of node $j \in \mathcal{V}$ if and only if $(i,j) \in \mathcal{E}$. When $(i,j) \in \mathcal{E}$ if and only if $(j,i) \in \mathcal{E}$, the graph is *undirected*. The in-neighbor set of node j is $\mathcal{N}_j = \{\, i \mid (i,j) \in \mathcal{E}\}$. For a graph with n nodes, we associate an adjacency matrix $W \in \mathbb{R}^{n\times n}$ with entries $w_{ij} \in \mathbb{R}_{\geq 0}$, where $w_{ij} = 0$ if and only if $(i,j) \notin \mathcal{E}$. For undirected graphs, the adjacency matrix is symmetric.

A path is a collection of nodes $\{i_1,\dots,i_\ell\} \subseteq \mathcal{V}$ such that $(i_k, i_{k+1}) \in \mathcal{E}$ for all $k \in [\ell-1]$. A digraph is *strongly connected* if there exists a path between any two nodes in $\mathcal{V}$. If the digraph is strongly connected, the adjacency matrix is irreducible. An undirected graph is *connected* if it contains a path between any two nodes in $\mathcal{V}$. A digraph is *weakly connected* if, when every edge in $\mathcal{E}$ is viewed as an undirected edge, the resulting graph is a connected undirected graph. A directed or undirected graph is *disconnected* if it contains at least two isolated subgraphs. Throughout, when $\mathcal{G}$ is directed, we assume it is either strongly or weakly connected; when $\mathcal{G}$ is undirected, we assume it is connected.

A. Compartmental Models and Their Stability Analysis

Compartmental models comprise separately identified segments of the population, which are assumed to reside in one of a fixed number of disease-states at each point in time. For these models, the *basic reproduction number* (BRN), often defined as a stability threshold denoted $\mathcal{R}_0$, serves as a metric that captures the "seriousness" of viral spread and is considered the fundamental threshold value in epidemiology [120]. The BRN $\mathcal{R}_0$ is the expected number of secondary infections arising from one individual throughout their entire infectious period, and it can be used to evaluate the effectiveness of an action aimed at mitigating the disease spread. To stop the spreading, we want $\mathcal{R}_0 < 1$; because of the nonlinear nature of spread dynamics we can also allow $\mathcal{R}_0 = 1$. We now introduce SIS, SIRS, and SAIRS model structures and evaluate the BRN thresholds in terms of their dynamic stability property.

1) SIS Model: The simplest compartmental model is the SIS model [3], given by

$$\begin{aligned} \dot{S}(t) &= -\beta S(t)I(t) + \gamma I(t), \\ \dot{I}(t) &= \beta S(t)I(t) - \gamma I(t), \end{aligned} \tag{7}$$

where $S(t)$ is the susceptible fraction of the population, $I(t)$ is the infected fraction, β represents the rate of infection, or contact between susceptible and infected segments of the population, and γ represents the healing or recovery rate of the population. The model assumes a homogeneous population with no vital dynamics (i.e., infection and healing are assumed to occur at faster rates than birth and death processes), and the population size is assumed to remain constant and mix over a trivial network, that is, over a complete graph structure. These statements imply $S(t) + I(t) = 1$; $\dot{S} + \dot{I} = 0$, and a certain percentage of those infected will become susceptible again (following recovery). SIS models capture the disease dynamics of recurrent bacterial and fungal infections.

For the SIS model (7), the BRN is given by $\mathcal{R}_0 = \beta/\gamma$, which is the ratio of the infection to healing rates. The disease-free equilibrium (DFE), with $I = 0$, is globally asymptotically stable if, and only if, $\mathcal{R}_0 \leq 1$. In fact, rewriting the second equation of (7) using the identity $S(t) = 1 - I(t)$ gives

$$\dot{I}(t) = \beta(1 - I(t))I(t) - \gamma I(t) = \gamma\left(\frac{\beta}{\gamma} - 1\right) I(t) - \beta I^2(t). \tag{8}$$

This differential equation is bounded above by the linearized subsystem; with the linear part zero (that is, when

$\mathcal{R}_0 = 1$) the nonlinear part alone leads to global asymptotic stability (GAS), and thus we have that $\mathcal{R}_0 \leq 1$ provides a sufficient condition for GAS (this holds from all initial conditions for I, but what is relevant is the system behavior for initial conditions $I(0) \in [0, 1]$). Necessity follows from the fact that when $\mathcal{R}_0 > 1$ the linear part is unstable.

When $\mathcal{R}_0 > 1$, the endemic state of the SIS model is

$$I^e = 1 - \frac{\gamma}{\beta} > 0.$$

Defining the equilibrium shifted variable $\tilde{I} := I - I^e$ leads to the differential equation (for $\tilde{I}$):

$$\dot{\tilde{I}} = -\beta I^e \tilde{I} - \beta \tilde{I}^2 \,,$$

and from a similar argument as above, it follows that $\tilde{I} = 0$ is globally asymptotically stable. Hence, translating to the original variable I, I^e is the globally asymptotically stable endemic equilibrium of the SIS model dynamics whenever $\mathcal{R}_0 > 1$ and $I(0) > 0$.

2) SIR Model: A slightly more complex model, in which an agent may remain in a state of complete recovery for some duration of time prior to returning to the susceptible state, is the SIR model [3], given by

$$\begin{aligned} \dot{S}(t) &= -\beta S(t) I(t) + \delta R(t), \\ \dot{I}(t) &= \beta S(t) I(t) - \gamma I(t), \\ \dot{R}(t) &= \gamma I(t) - \delta R(t), \end{aligned} \tag{9}$$

where β is the transmission rate parameter for person-to-person contact, γ is the recovery rate, δ is the rate at which immunity recedes following recovery, and $R(t)$ is the recovered fraction of the population. Precisely, this is an SIRS model, used when acquired immunity is only temporary, as e.g. with noroviruses and some common cold viruses; setting $\delta = 0$ gives an SIR model, used for the dynamics of diseases for which permanent acquired immunity results following infection, as e.g. with measles or mumps.

For the SIRS model (9), again $\mathcal{R}_0 = \beta/\gamma$. In fact, the same approach as in (8) for the SIS model leads to two coupled differential equations:

$$\begin{aligned} \dot{I} &= -(\gamma - \beta) I - \beta R I - \beta I^2, \\ \dot{R} &= \gamma I - \delta R. \end{aligned} \tag{10}$$

When $\delta > 0$, the DFE is $I^e = R^e = 0$, $S^e = 1$ (eventually all recovered become susceptible again, and now remain susceptible since $I^e = 0$). Linearizing around this DFE leads to the Jacobian matrix

$$J^e = \begin{bmatrix} \beta - \gamma & 0 \\ \gamma & -\delta \end{bmatrix},$$

which is Hurwitz if and only if $\beta - \gamma < 0$ (i.e., $\mathcal{R}_0 < 1$) and $\delta > 0$. This condition also leads to GAS of the DFE since the two nonlinear terms in the differential equation for I are negative, driving I to zero globally, which also drives R to zero because of the $-\delta R$ term.

If $\delta = 0$, we cannot use the same argument for linearization around $I = R = 0$, since there is now no positive feedback term from the R group to S group. However, for comparison, assume for the moment that linearization around $I = R = 0$ makes sense, which is valid when δ is very small and positive, and hence one can consider SIR stability as a limiting case of SIRS stability. Again the Hurwitz condition is satisfied if and only if $\beta - \gamma < 0$, i.e. $\mathcal{R}_0 < 1$. This condition also leads to GAS by the argument used in the SIRS case. In this case we can let $\mathcal{R}_0 = 1$ and establish GAS of the DFE, since $\dot{I} = -\beta R I - \beta I^2$; with R being nonnegative, we have GAS.

As a further result of linearization, if $\mathcal{R}_0 > 1$, then for each respective model the DFE is unstable.

Returning to the DFE for the SIR model (with $\delta = 0$), we have the coupled ODEs:

$$\begin{aligned} \dot{I} &= -(\gamma - \beta) I - \beta R I - \beta I^2, \\ \dot{R} &= \gamma I. \end{aligned} \tag{11}$$

The equilibrium state in this case is $I^e = 0$, $R^e = 1$,[1] with R positive throughout, except for $I(0) = 0$, and the right-hand-side of the ODE for I negative whenever $I(0) \neq 0$, and $\mathcal{R}_0 \leq 1$; hence, the DFE is GAS if and only if $\mathcal{R}_0 \leq 1$.

Conversely, when $\mathcal{R}_0 > 1$, there is no endemic equilibrium, because if the right hand side of the equation for I in (11) is set to zero, for $I \neq 0$ it leads to $I = 1 - R - (\gamma/\beta)$, which is positive only if $R + (\gamma/\beta) < 1$, but there is no such limiting R value since R increases with positive I.

For SIRS, setting the right-hand-sides of the coupled ODEs in (10) equal to zero leads to a unique solution (for $I \neq 0$):

$$R^* = \frac{\gamma(\beta - \gamma)}{\beta(\gamma + \delta)}, \qquad I^* = \frac{\delta(\beta - \gamma)}{\beta(\gamma + \delta)}$$

which are both positive whenever $\mathcal{R}_0 > 1$. Since $I^* + R^* = 1 - (\gamma/\beta)$, the endemic equilibrium state of S is independent of δ. See [8] and the references therein for further discussions on stability and endemic equilibria of SIS and SIR models.

3) SEIR and SAIR Model: To explicitly capture the incubation period from time of exposure to the virus, to the time that symptoms and associated viral shedding are present, an SEIR (or SEIRS) model may be used. Allowing that the recovered population may become susceptible again after a period of immunity, we have the SEIRS model:

$$\begin{aligned} \dot{S}(t) &= -\beta S(t) I(t)) + \delta R(t), \\ \dot{E}(t) &= \beta S(t) I(t)) - \sigma E(t), \\ \dot{I}(t) &= \sigma E(t) - \gamma I(t), \\ \dot{R}(t) &= \gamma I(t) - \delta R(t), \end{aligned} \tag{12}$$

where β is the transmission rate from agent-to-agent contact between susceptible and infected, after which the agent is considered exposed, σ is the transition rate from exposed to infected, γ is the recovery rate, and δ represents the rate at which immunity recedes.

The SEIR(S) model captures the delay between time of exposure and when an agent becomes simultaneously

[1] This not an equilibrium state in the true sense of the notion, since once $R = 1$ it stays there, which is not captured by the smooth right-hand-side of the differential equation above.

symptomatic and infectious, but does not capture disease spread by infectious but asymptomatic agents. For COVID-19, the SEIR models have been adapted to reflect the state of being both asymptomatic and infectious, leading to the SAIRS compartment model:

$$\begin{array}{rcl} \dot{S}(t) &=& -\beta S(t)(A(t)+I(t)) + \delta R(t), \\ \dot{A}(t) &=& \beta q S(t)(A(t)+I(t)) - \sigma A(t) - \kappa A(t), \\ \dot{I}(t) &=& \beta(1-q) S(t)(A(t)+I(t)) + \sigma A(t) - \gamma I(t) \\ \dot{R}(t) &=& \kappa A(t) + \gamma I(t) - \delta R(t), \end{array} \tag{13}$$

where β is the rate of infection or contact, now amongst susceptible, asymptomatic-infected and infected-symptomatic individuals; σ is the rate of progression from asymptomatic to symptomatic infected; κ and γ are the recovery rates for asymptomatic and infected-symptomatic individuals, respectively; δ is the rate at which recovered individuals become susceptible again (i.e., lose acquired immunity to the disease) and $\delta = 0$ if the acquired immunity is permanent. The SAIR model captures the case of being both asymptomatic and infectious, and possibly recovering without ever exhibiting symptoms. The parameter q, and the $(1-q)$ term, represent the probabilities (or fractions) of susceptible individuals transitioning, respectively, to A and I states from S. These models may be further generalized, e.g., by allowing for different β values between S and A states, and S and I states. No general vital dynamics are included in these models, thus $S(t) + A(t) + I(t) + R(t) = 1$.

While (13) models the type of asymptomatic-but-infectious state that may occur e.g. with COVID-19, there are other variations on SAIR model structures, such as those first proposed by [121] for dengue virus epidemics, where being asymptomatic one year may lead to more severe infections from dengue virus strains in following years.

To consider its stability, by using $S(t) = 1 - A(t) - I(t) - R(t)$, the SAIRS model (13) can be written as

$$\begin{array}{rcl} \dot{A}(t) &=& q\beta(1-A(t)-I(t)-R(t))(A(t)+I(t)) \\ && -\sigma A(t) - \kappa A(t) \\ \dot{I}(t) &=& (1-q)\beta(1-A(t)-I(t)-R(t))(A(t)+I(t)) \\ && +\sigma A(t) - \gamma I(t) \\ \dot{R}(t) &=& \kappa A(t) + \gamma I(t) - \delta R(t). \end{array} \tag{14}$$

Assuming $\delta > 0$ we consider linearization about the DFE point at $A^e = I^e = R^e = 0$, $S^e = 1$, which implies that all recovered become susceptible again and remain susceptible since $I^e = 0$; this gives us the Jacobian matrix

$$J^e = \begin{bmatrix} \beta q - \sigma - \kappa & \beta q & 0 \\ \beta(1-q) + \sigma & \beta(1-q) - \gamma & 0 \\ \kappa & \gamma & -\delta \end{bmatrix}.$$

Applying [122, Theorem 4.7], eigenvalue analysis and the Routh-Hurwitz criterion shows that the SAIRS model is GAS at the DFE when

$$\mathcal{R}_0 := \max\left(\frac{\beta}{\gamma + \sigma + \kappa}, \frac{\beta(q\gamma + (1-q)\kappa + \sigma)}{\gamma(\sigma + \kappa)} \right) < 1.$$

We can further compute an endemic equilibrium point for (14), strictly assuming non-permanent immunity: $\delta > 0$. Setting $\dot{A}(t), \dot{I}(t), \dot{R}(t)$ to 0, we obtain the endemic equilibrium, which can be written as

$$\begin{bmatrix} S^e \\ A^e \\ I^e \\ R^e \end{bmatrix} = \begin{bmatrix} \frac{\Psi}{\beta\Phi} \\ \frac{q\delta\gamma(\beta\Phi - \Psi)}{\beta\Phi(\delta\Phi + \Psi)} \\ \frac{\delta((1-q)\kappa + \sigma)(\beta\Phi - \Psi)}{\beta\Phi(\delta\Phi + \Psi)} \\ \frac{\Psi(\beta\Phi - \Psi)}{\beta\Phi(\delta\Phi + \Psi)} \end{bmatrix} = \begin{bmatrix} \frac{\Psi}{\beta\Phi} \\ \frac{q\delta\gamma C}{\beta\Phi D} \\ \frac{\delta((1-q)\kappa + \sigma)C}{\beta\Phi D} \\ \frac{\Psi C}{\beta\Phi D} \end{bmatrix} \tag{15}$$

by denoting $\Psi = \gamma(\kappa + \sigma)$ and $\Phi = q\gamma + (1-q)\kappa + \sigma$, where both $\Psi > 0$ and $\Phi > 0$, and further defining $C = \beta\Phi - \Psi = \beta(q\gamma + (1-q)\kappa + \sigma) - \gamma(\kappa + \sigma)$ and $D = \delta\Phi + \Psi = \delta(q\gamma + (1-q)\kappa + \sigma) + \gamma(\kappa + \sigma) > 0$.

Then, computing the Jacobian around the equilibrium

$$\begin{bmatrix} -\frac{(\kappa+\sigma)\left((1-q)\kappa+\sigma\right)}{\Phi} - \frac{q\delta C}{D} & \frac{q\Psi}{\Phi} - \frac{q\delta C}{D} & -\frac{q\delta C}{D} \\ \frac{(\gamma+\sigma)\left((1-q)\kappa+\sigma\right)}{\Phi} - \frac{(1-q)\delta C}{D} & -\frac{q\gamma(\gamma+\sigma)}{\Phi} - \frac{(1-q)\delta C}{D} & -\frac{(1-q)\delta C}{D} \\ \kappa & \gamma & -\delta \end{bmatrix}.$$

allows us to derive global asymptotic stability conditions by applying the Routh-Hurwitz criterion.

B. Networked Models

Networked models capture the scenario where numerous groups, or agents, are interconnected via a contact graph or a more general interconnection network, defined by a weighted adjacency matrix, $W = \{w_{ij}\}$, where element w_{ij} quantifies the strength of the connection from agent j to agent i. If we assume as before large and constant population sizes (and some independence conditions), then compartment models can be extended to describe the dynamics of epidemic processes evolving over networks of subgroups or agents in the population.

For networked models, we can also derive threshold values that play an important role in characterizing stability of the spread dynamics around equilibria. Now the thresholds admit the interpretation of being the expected number of healthy agents or nodes in a susceptible population that become infected due to the state of infection at neighboring nodes.

1) SIS Model: Denoting by $p_i(t) \in [0,1]$ the fraction of the subpopulation at node i infected at time t, or the probability of node i being infected at any time t, we can derive the following differential equation representing the evolution of the p_i's, for $i \in [n]$,

$$\dot{p}_i(t) = (1 - p_i(t))\beta \sum_{j=1}^{n} w_{ij} p_j(t) - \gamma p_i(t)\,, \tag{16}$$

where $\beta > 0$ and $\gamma > 0$ are as defined previously, and w_{ij} are the non-negative edge weights between the agents/nodes.

One way to derive the model in (16) is to use a mean field approximation of a 2^n state Markov chain model that captures the networked SIS dynamics. Specifically consider the 2^n-state Markov chain [68] where each state of the chain, $Y_k(t)$, corresponds to a binary-valued string x of length n, where the ith agent is either infected or susceptible, indicated by $x_i = 1$ or $x_i = 0$, respectively, and the state transition matrix, $\bar{Q}$, is defined by

$$\bar{q}_{kl} = \begin{cases} \gamma, & \text{if } x_i = 1, k = l + 2^{i-1} \\ \beta \sum_{j=1}^{n} w_{ij} x_j, & \text{if } x_i = 0, k = l - 2^{i-1} \\ -\sum_{l \neq j} \bar{q}_{jl}, & \text{if } k = l \\ 0, & \text{otherwise,} \end{cases} \tag{17}$$

for $i \in [n]$. Here a virus is propagating over a network structure defined by w_{ij}, with n agents or possibly n groupings of agents; β and γ are the homogeneous (same for each node) infection and healing rate, respectively. The state vector $y(t)$ is defined by

$$y_k(t) = Pr[Y_k(t) = k], \tag{18}$$

with $\sum_{k=1}^{2^n} y_k(t) = 1$. The Markov chain evolves according to

$$\frac{dy^\top(t)}{dt} = y^\top(t)\bar{Q}. \tag{19}$$

Alternatively, let $X_i(t)$ be the random variable representing whether the ith agent is infected or not (while x_i is the ith entry of the binary string associated with each state of the 2^n Markov chain), and consider the probabilities associated with node i being healthy ($X_i = 0$) or infected ($X_i = 1$) at time $t + \Delta t$, given $X_i(t)$:

$$Pr(X_i(t+\Delta t) = 0 | X_i(t) = 1, X(t)) = \gamma \Delta t + o(\Delta t),$$
$$Pr(X_i(t+\Delta t) = 1 | X_i(t) = 0, X(t)) = \beta \textstyle\sum_{j=1}^{n} w_{ij} X_j \Delta t + o(\Delta t).$$

Letting Δt go to zero and taking expectations gives us

$$\dot{E}(X_i(t)) = E\left((1 - X_i(t)) \beta \sum_{j=1}^{n} w_{ij} X_j(t) \right) - \gamma E(X_i(t)). \tag{20}$$

Using the above equation, the identities $Pr(z) = E(1_z)$, $p_i(t) = Pr(X_i(t) = 1)$, $(1 - p_i(t)) = Pr(X_i(t) = 0)$, and approximating $Pr(X_i(t) = 1, X_j(t) = 1)$ by $p_i(t)p_j(t)$ (which inaccurately assumes independence) gives (16).

For both interpretations of the model to be well defined, each state $p_i(t)$ must remain in the domain $[0, 1]$ for all $t \geq 0$. This well-posedness result is straightforward to show.

Lemma 2: If $p_i(0) \in [0, 1]$, for all $i \in [n]$, then $p_i(t) \in [0, 1]$, for all $t \geq 0$, $i \in [n]$.

To perform a stability analysis, we first recall the general network structure, also known as the *n-intertwined Markov model*.

Following [123], we describe the networked SIS infection model over a directed graph (digraph) $\mathcal{G} = (\mathcal{V}, \mathcal{E})$ with n nodes, where $\mathcal{V}$ is the set of nodes, and $\mathcal{E}$ is the set of edges. Each node in the network has two states: infected or cured. The curing and infection of a given node $i \in \mathcal{V}$ are described by two independent Poisson processes with rates γ_i and β_i, respectively. Throughout, we assume that $\gamma_i > 0$ and $\beta_i > 0$. The transition rates between the healthy and infected states of a given node's Markov chain depend on its curing rate as well as the infection probabilities among its neighbors. A mean-field approximation is introduced to "average" the effect of infection probabilities of the neighbors on the infection probability of a given node. This approximation yields a dynamical system that describes the evolution of the probability of infection of node $i \in \mathcal{V}$, as described next.

Let $p_i(t) \in [0, 1]$ be the infection probability of node $i \in \mathcal{V}$ at time $t \geq 0$, and let $p(t) = [p_1(t), \ldots, p_n(t)]^\top$. Also, let $\Gamma = \text{diag}(\gamma_1, \ldots, \gamma_n)$, $P(t) = \text{diag}(p(t))$, and $B = \text{diag}(\beta_1, \ldots, \beta_n)$. The n-intertwined Markov model is prescribed by the mapping $\Phi : \mathbb{R}^n \to \mathbb{R}^n$, where

$$\dot{p}(t) = \Phi(p(t)) := (W^\top B - \Gamma)p(t) - P(t)W^\top B p(t). \tag{21}$$

When $p(0) \in [0, 1]^n$, $p(t) \in [0, 1]^n$, for all $t > 0$.

We characterize the set of equilibria of the dynamical system (21) in terms of the *basic reproduction number* (BRN), denoted by $\mathcal{R}_0$, introduced earlier in the context of the compartmental SIS model, whose counterpart in the case of networked SIS as above is the expected number of infected nodes produced in a completely susceptible population due to the infection of a neighboring node. For the n-intertwined Markov model, the BRN is $\mathcal{R}_0 = \rho(\Gamma^{-1}W^\top B)$ [124]. For connected undirected graphs, the DFE is the unique equilibrium for the n-intertwined Markov model when $\mathcal{R}_0 \leq 1$; when $\mathcal{R}_0 > 1$, in addition to the disease-free equilibrium, an endemic equilibrium, denoted by $p^\star$, emerges [68]. In fact, it is shown that $p^\star \gg 0$. We call a strictly positive endemic state *strong*. When $p^\star > 0$, we call it a *weak* endemic state. A recursive expression for the endemic state $p^\star$ is provided in [124], which is shown to depend on the problem parameters only: W, γ_i, β_i, $i \in \mathcal{V}$. The steady-state equation evaluated at $p^\star$ is given by

$$W^\top B p^\star = (I - P^\star)^{-1} \Gamma p^\star, \tag{22}$$

where $P^\star = \text{diag}(p^\star)$. Since $\gamma_i > 0$, then $p_i^\star < 1$, for all $i \in \mathcal{V}$, and $(I - P^\star)^{-1}$ exists.

A necessary and sufficient condition for the stability of the disease-free equilibrium is given in the following proposition.

Proposition 1: [70], [125] Suppose $\mathcal{G} = (\mathcal{V}, \mathcal{E})$ is a strongly connected digraph. The DFE of (16) is asymptotically stable with domain of attraction $[0, 1]^n$ if and only if $\mathcal{R}_0 \leq 1$.

The BRN provides a sharp threshold for the stability of the disease-free equilibrium, as in the compartmental SIS model. Further results when $\mathcal{G}$ is not strictly assumed to be a digraph, and when the network interconnection structure may be time-varying, are in [18] and [71], respectively.

To provide concrete results on local and global asymptotic stability of an endemic state over strongly connected digraphs, we first note the existence of a unique endemic state for (21).

Proposition 2: [70] Let $\mathcal{G} = (\mathcal{V}, \mathcal{E})$ be a strongly connected digraph. Then, a unique strong endemic state $p^\star \gg 0$ exists if and only if $\mathcal{R}_0 > 1$.

The following result on stability of the endemic state is proven by using positive systems theory and properties of Metzler matrices (a real square matrix X is *Metzler* if its off-diagonal entries are nonnegative).

Theorem 2: [123] Let $\mathcal{G} = (\mathcal{V}, \mathcal{E})$ be a strongly connected

digraph, and assume that $p(0) \neq 0$. If $\mathcal{R}_0 > 1$, then the strong endemic state $p^\star$ is globally asymptotically stable, with convergence being exponential locally.

Global stability of the endemic equilibrium was recently shown under slightly stronger assumptions [126]. Considering multiple virus strains over multi-layer networks leads to notably more complex stability conditions [78], [127].

2) SIR Model: Denoting the probability of node i being infected by $p_i(t) \in [0,1]$ and being recovered by $r_i(t) \in [0,1]$, respectively at any time t, we obtain the following differential equations governing the evolution of the p_i's and r_i's:

$$\begin{array}{rcl} \dot{p}_i & = & (1-p_i-r_i)\beta \sum_{j=1}^n w_{ij} p_j - \gamma p_i, \\ \dot{r}_i & = & \gamma p_i. \end{array} \tag{23}$$

For the networked SIR model to be well defined, the states and their sum must remain in $[0,1]$, which is again straightforward to show. Extensions of the SIS subpopulation derivation to the SIR model are in [128], [129].

To analyze stability, we first consider the continuous time model in (23). We appeal to a result by [17] which assumes homogeneous virus spread. Recall that $s_i(t) = 1 - p_i(t) - r_i(t)$ for all $i \in [n]$.

Theorem 3: [17] Consider the model in (23) with homogeneous spread, $\beta > 0$, $\gamma > 0$, W irreducible, $p_i(0) > 0$ for some i, and $s_i(0) > 0$ for all $i \in [n]$. For $t \geq 0$, let $\lambda_{\max}(t)$ and $v_{\max}(t)$ be the dominant eigenvalue of the non-negative matrix $\mathrm{diag}(s(t))W$ and the corresponding normalized left eigenvector, respectively. Then, for all $i \in [n]$,

i) $t \to s_i(t)$ is monotonically decreasing, for all $t \geq 0$,
ii) the set of equilibrium points is the set of pairs $(s^*, \mathbf{0})$, for any $s^* \in [0,1]^n$,
iii) $\lim_{t\to\infty} p_i(t) = 0$,
iv) there exists $\bar{t}$ such that $\beta\lambda_{\max}(t) < \gamma$ for all $t \geq \bar{t}$, and the weighted average $t \to v_{\max}(\bar{t})^\top x(t)$, for $t \geq \bar{t}$, is monotonically and exponentially decreasing to zero.

3) SAIR Model: Model (13) can also be extended to reflect contact network structures. Assuming heterogeneous infection, healing, and transition rates for each of the network nodes yields

$$\begin{array}{l} \dot{s}_i(t) = -\beta_i s_i(t) \left(\sum_{j=1}^n w_{ij}(a_j(t) + p_j(t)) \right) + \delta_i r_i(t) \\ \dot{a}_i(t) = \beta_i q s_i(t) \left(\sum_{j=1}^n w_{ij}(a_j(t) + p_j(t)) \right) - (\sigma_i + \kappa_i) a_i(t) \\ \dot{p}_i(t) = \beta_i (1-q) s_i(t) \left(\sum_{j=1}^n w_{ij}(a_j(t) + p_j(t)) \right) + \sigma_i a_i(t) - \gamma_i p_i(t) \\ \dot{r}_i(t) = \kappa_i a_i(t) + \gamma_i p(t) - \delta_i r_i(t) \end{array} \tag{24}$$

Here, $s_i(t)$ and $a_i(t)$ may be the probabilities of individual i, or the fractions of the subpopulation i, being respectively susceptible or asymptomatic at a given time t, and $p_i(t)$ and $r_i(t)$ are interpreted the same as in the SIR model. The parameters are as defined for the compartmental SAIR model. Note that $s_i(t) = 1 - a_i(t) - p_i(t) - r_i(t)$ for all $i \in [n]$, and the usual well-posedness result can be stated, which we now provide in the most general form:

Lemma 3: Consider the model in (24) and assume for all $i, j \in [n]$, we have $\beta_i,\ \gamma_i,\ \delta_i,\ \sigma_i,\ \delta_i,\ w_{ij} \geq 0$, $0 \leq q \leq 1$. Suppose $s_i(0), a_i(0), p_i(0), r_i(0) \in [0,1]$, and $s_i(0) + a_i(0) + p_i(0) + r_i(0) = 1$ for all $i \in [n]$. Then, for all $t \geq 0$ and $i \in [n]$, we have $s_i(t), a_i(t), p_i(t), r_i(t) \in [0,1]$ and $s_i(t) + a_i(t) + p_i(t) + r_i(t) = 1$.

We now evaluate equilibria and their stability properties for the networked SAIR(S) models. First we consider the case with permanent immunity, i.e., $\delta = 0$. Given $s_i(t) = 1 - a_i(t) - p_i(t) - r_i(t)$ for all $t \geq 0,\ i \in [n]$, the system can be represented in matrix form as:

$$\begin{array}{rcl} \dot{a}(t) & = & [q(I - A(t) - P(t) - R(t))BW - \Sigma - K]a(t) \\ & & +q(I - A(t) - P(t) - R(t))BWp(t) \\ \dot{p}(t) & = & [(1-q)(I - A(t) - P(t) - R(t))BW + \Sigma]a(t) \\ & & +[(1-q)(I - A(t) - P(t) - R(t))BW - \Gamma]p(t) \\ \dot{r}(t) & = & Ka(t) + \Gamma p(t) - \Delta r(t), \end{array} \tag{25}$$

with $a(t) = [a_1(t), \ldots, a_n(t)]^\top$, $p(t) = [p_1(t), \ldots, p_n(t)]^\top$, $r(t) = [r_1(t), \ldots, r_n(t)]^\top$, and $n \times n$ matrices $A(t) = \mathrm{diag}(a_i(t))$, $P(t) = \mathrm{diag}(p_i(t))$, $R(t) = \mathrm{diag}(r_i(t))$, $B = \mathrm{diag}(\beta_i)$, $K = \mathrm{diag}(\kappa_i)$, $\Gamma = \mathrm{diag}(\gamma_i)$, $\Sigma = \mathrm{diag}(\sigma_i)$, $\Delta = \mathrm{diag}(\delta_i)$, and adjacency matrix W.

Setting $\dot{a}(t)$, $\dot{p}(t)$, $\dot{r}(t)$ to 0, we can compute the equilibrium state where $a^e = p^e = \overline{0}$, $r^e = \overline{r_c}$, where $\overline{r_c}$ is any non-negative constant vector with elements $r_{c_i} < 1$. Linearizing the system (25) at the equilibrium (a^e, p^e, r^e), we obtain the $3n \times 3n$ system Jacobian matrix, J^e, given by

$$\begin{bmatrix} q(I-R_c)BW - \Sigma - K & q(I-R_c)BW & 0 \\ (1-q)(I-R_c)BW + \sigma & (1-q)(I-R_c)BW - \Gamma & 0 \\ K & \Gamma & -\Delta \end{bmatrix},$$

whose analysis leads to a set of constraints on the spectrum of the weighting matrix W. An alternative Lyapunov stability analysis approach leverages a quadratic Lyapunov function $V = a^\top B^{-1} a + p^\top B^{-1} p$, for which

$$\dot{V} \leq a^\top [qW - B^{-1}(\Sigma + K)]a + p^\top [(1-q)W - b^{-1}\Gamma]p + a^\top (W + B^{-1}\Sigma)p. \tag{26}$$

For GAS, we require $\dot{V} < 0$ for all $t \geq 0$, which after the application of the Rayleigh quotient leads us to the following sufficient condition for the DFE.

Theorem 4: For the system (25), the DFE $(a^e, p^e, r^e) = (0, 0, \overline{r_c})$ is globally asymptotically stable (GAS) when

$$\begin{bmatrix} qW & \frac{1}{2}W \\ \frac{1}{2}W & (1-q)W \end{bmatrix} \prec \begin{bmatrix} B^{-1}(\Sigma + K) & -\frac{1}{2}B^{-1}\Sigma \\ -\frac{1}{2}B^{-1}\Sigma & B^{-1}\Gamma \end{bmatrix}, \tag{27}$$

where $\prec$ denotes relative definiteness of the matrices.

The theorem provides a test that bounds the maximum eigenvalue of the q-scaled adjacency matrix W in terms of the minimum eigenvalue of a matrix consisting of diagonal block entries of ratios of healing and transition rates (κ_i, γ_i and σ_i) to infection rates (β_i); this generalizes the R_0 threshold to allow for heterogeneous infection parameters over multiple infection compartments, in the networked SAIRS model.

Remark 5: For a slightly simpler spread process model, e.g. a networked SIRS model, a sufficient condition for convergence to the DFE is $\lambda_{\max}(W) < \lambda_{\min}(B^{-1}\Gamma) = \min_i(\gamma_i/\beta_i) = \min_i(1/R_{0_i})$.

IV. Holistic Models and Multi-Pronged Interventions to Contrast Epidemics

We adopt here a holistic approach aimed at integrating interdisciplinary perspectives into epidemiological models, so as to be able to design optimal approaches to manage epidemics also in the presence of possibly conflicting multi-objective goals, related e.g. to public health, social and psychological well-being, economic growth. We discuss approaches to design effective interventions to contain the epidemic spread, with a special focus on optimal control, and we highlight the importance of taking into account human behaviour, which is influenced by the epidemic evolution and at the same time affects the spread of the contagion depending on the individual adherence to restrictions and to vaccination, based on opinions and beliefs that evolve according to the available information. We then illustrate multi-scale epidemiological models that bridge the microscopic, immunological scale dissected by in-host models in Section II and the macroscopic, epidemiological scale captured by the between-host models in Section III. The complexity and relevance of enabling the design of coordinated epidemic control across scales make multi-scale epidemiological modelling a challenging and fascinating research direction [130].

A. Modelling the Effect of Containment Measures

The multifaceted types of pharmaceutical and non-pharmaceutical interventions that can be adopted [33] to contrast the spread of an infectious disease can be embedded in the models in multiple ways. The most common NPI is the quarantine of diagnosed infected individuals, which can be modelled by including specific compartments in the epidemic model [14], [15], [131]; if a non-negligible fraction of infected population is undetected, or diagnosed with delay, non-diagnosed groups are included in the models [15]. Then, the transmission rate for contacts between a susceptible and a non-quarantined infected is much higher than the transmission rate for contacts between a susceptible and a quarantined infected. Preventive quarantine of the whole population (namely, lockdown) is the most extreme measure in terms of physical distancing [132]. The effect of tightening and loosening such measures can be modelled by enforcing time-varying transmission parameters in epidemic models [15], [41], [133]: in the models discussed in Section III, the transmission rate β is thus replaced by a time-varying $\beta(t)$, which can also be written as $\beta - u(t)$ to emphasise the role of the control. Also demographic properties of a given population and seasonality of some diseases lead to an (uncontrolled) time-varying infection rate [134], [135].

Governments often introduce long-range travel bans or local mobility restrictions that are effectively captured by *multi-patch* or *meta-population* models, accounting for the heterogeneity of the epidemic evolution in distinct geographical areas, or different age classes, and for the mobility of individuals [136]–[140]. In these networked models, each node represents the local dynamic evolution of the epidemic phenomenon, typically through a compartmental model, and the interconnections represent population mobility that couples contagion dynamics at a larger scale. Capturing the hierarchical levels of the epidemic phenomenon at various spatial scales (city, province, region, country, continent) is crucial to plan coordinated interventions with a national or continental perspective [52], [53]. Epidemiological models with a spatial structure can show how mobility restrictions influence the final size of the outbreak [141].

Mass testing, along with contact tracing that aims at identifying and isolating infected individuals by following the contact network of detected infected [83], [142], can also be represented by explicitly including diagnosed and non-diagnosed compartments in epidemic models: a higher level of testing and tracing is then represented in terms of a larger rate of diagnosis associated with the flow from the non-diagnosed to the diagnosed compartments [15]. Diagnosis is beneficial also because detected infected are less likely to transmit the disease due to the adopted precautions.

The controllability of an epidemic highly depends on the reproduction number [2], [143] discussed in Section III: in homogeneously mixed communities, epidemics can be prevented by keeping below 1 the *effective reproduction number* $\mathcal{R}(t) = S(t)\mathcal{R}_0$, which quantifies the average number of secondary infections per infectious case in a population with both susceptible and non-susceptible hosts, and hence the effectiveness of the adopted interventions. If $\mathcal{R}(t) < 1$, then the incidence of new infections decreases and the spread of contagion diminishes over time, leading to convergence to the DFE. In the SIS and SIR case, $\mathcal{R}(t) = S(t)\frac{\beta}{\gamma}$ is the product of the size of the susceptible population $S(t)$, the transmission rate β, and the mean duration of the infectious period $1/\gamma$. NPIs aim at reducing β by limiting human-to-human contacts that may lead to contagion. Improving therapies by devising new drugs and treatment strategies can reduce the duration of the infectious period, i.e. increase the recovery rate γ. The fraction of susceptible individuals can be reduced e.g. by vaccination [16] or by repeated waves of infection over the years [144]. Clearly, the duration of the acquired immunity (either due to a vaccine or to past infections) is critical, as for example in the case of the COVID-19 pandemic, and waning immunity needs to be considered when modelling mid/long-term epidemic evolution [58].

B. Optimal Control Theory

Several epidemiological problems, including the control of infectious diseases such as rabies [54] and tuberculosis [145], benefit from optimal control approaches, which, together with a qualitative analysis of the epidemic model, can provide useful insights to manage large-scale outbreaks and reduce the epidemic burden [34]–[50].

The dynamic optimisation techniques of the calculus of variations and of optimal control theory provide methods for solving problems in continuous time and identifying a suitable strategy to control the system and achieve a desired outcome, expressed by the minimisation of a cost function subject to constraints. The corresponding solution is a continuous function (or a set of functions) indicating the

optimal path to be followed by the variables through time or space. In a standard optimal control formulation

$$\begin{aligned} &\min_{y,u} J(y,u) = \int_0^T \ell(y(t),u(t),t)dt + g(y(T)) \\ &\dot{y} = f(t,y(t),u(t)) \quad \text{for } t \in (0,T) \\ &y(0) = y_0 \\ &u \in U_{ad} \end{aligned} \tag{28}$$

with running cost $\ell(y(t),u(t),t)$ and terminal cost $g(y(T))$, applied to epidemic control, vector $y(t)$ stacks the population fractions in the different compartments at a given time t, $u(t)$ is the control function, which can be e.g. the vaccination rate or the modified infection rate, while the differential equation $\dot{y} = f(t,y(t),u(t))$ is the epidemic model, which could be e.g. SIR or SEIR, or more complex. The initial condition is y_0 and the control action $u(t)$ can be chosen from the admissible set of controls U_{ad}, where suitable constraints on the control action can express e.g. a limitation on the number of vaccine doses provided to a hospital per day or on the quantity of pharmacological treatment provided to a patient. Finite horizon problems are mostly considered: the epidemic situation is strongly time-varying and needs to be re-assessed periodically. Running costs are typically quadratic in both state and control, or linear in the state and quadratic in the control [50], but can also be linear in both state and control, or quadratic in the state and linear in the control [41].

The existence of at least one control function that solves (28) depends on the chosen model and constraints, and on the functional space where the control is sought [146], [147]. Once existence is guaranteed, Pontryagin's maximum principle yields a set of necessary conditions that characterise the optimal solutions [148] and become also sufficient under certain convexity conditions on the objective and constraint functions [149]. To derive this optimality system, the Hamilton-Pontryagin function $\mathcal{H}(t,y,u,p) = p \cdot f(t,y,u) + \ell(t,y,u)$ has to be defined, where p is the unique solution to the corresponding adjoint system [150].

We now illustrate some epidemiological optimal control problems; see [50] for further models and information.

1) Optimal control in SIR model with vaccination: Consider the SIRV model with the vaccinated compartment V

$$\begin{aligned} \dot{S}(t) &= b - \beta S(t)I(t) - au(t)S(t) - \mu S(t), \\ \dot{I}(t) &= \beta[S(t) + \epsilon V(t)]I(t) - \gamma I(t) - \mu I(t), \\ \dot{R}(t) &= \gamma I(t) - \mu R(t), \\ \dot{V}(t) &= au(t)S(t) - \beta\epsilon V(t)I(t) - \mu V(t), \end{aligned}$$

where b is the birth rate, μ is the basal death rate, β and γ are the transmission and healing rates, $\epsilon \in [0,1)$ expresses the reduced risk of contagion for vaccinated people, $u(t)$ is the controlled vaccination rate, with $0 \le u(t) \le 1$, and the initial conditions are $S(0) > 0$ and $I(0), R(0), V(0) \ge 0$. In the cost functional

$$J(y,u) = \int_0^T \left(\alpha_1 I(t) + \frac{\alpha_2}{2}u^2(t)\right) dt, \quad \alpha_1 > 0,$$

the term $\alpha_1 I(t)$ represents the cost of infections (related to the burden on the healthcare system, hospital beds, ICU beds, deaths), while the term $\frac{\alpha_2}{2}u^2(t)$ represents the cost of the vaccination program at time t (vaccine doses, logistics, implementation costs). When $u(t)$ is close to 1, then the vaccination campaign proceeds at full speed, but with high implementation costs.

2) Optimal control in SEIR model with quarantine and hospitalisation: Consider the SEQIHR model with quarantined compartment Q and hospitalised compartment H

$$\begin{aligned} \dot{S}(t) &= b + \rho Q(t) - \beta S(t)[I(t) + \epsilon_Q Q(t) + \epsilon_H H(t)] - \mu S(t) \\ \dot{E}(t) &= \beta S(t)[I(t) + \epsilon_Q Q(t) + \epsilon_H H(t)] - \gamma E(t) - \mu E(t) \\ \dot{Q}(t) &= u_1(t)\kappa\gamma E(t) - \eta Q(t) - \rho Q(t) - \mu Q(t) \\ \dot{I}(t) &= [1 - u_1(t)\kappa]\gamma E(t) - \alpha I(t) - \mu I(t) \\ \dot{H}(t) &= u_2(t)\nu\alpha I(t) + \eta Q(t) - \sigma H(t) - \mu H(t) \\ \dot{R}(t) &= [1 - u_2(t)\nu]\alpha I(t) + \sigma H(t) - \mu R(t) \end{aligned}$$

(the reader is referred to [50] for more details on the model parameters), with control functions $u_i(t)$, $0 \le u_i(t) \le 1$, for $i = 1, 2$, and a cost functional given by

$$J(y,u_1,u_2) = \int_0^T \left(\alpha_1 Q(t) + \alpha_2 I(t) + \alpha_3 H(t) + \frac{\alpha_4}{2}u_1^2 + \frac{\alpha_5}{2}u_2^2\right) dt,$$

with $\alpha_i > 0$. The control function $u_1(t)$ represents the fraction of asymptomatic infected that are identified and then quarantined, while $u_2(t)$ represents the fraction of symptomatic infected that are detected and hence hospitalised.

As shown by the above examples, epidemiological control problems are often characterised by nonlinear dynamics and control constraints. Thus, computing the solution requires numerical methods able to solve the above optimality system, also called Hamiltonian system: a two-point boundary value problem, plus a minimum condition of the Hamilton-Pontryagin function [150]. The most popular algorithm used in epidemiological control is the forward-backward-sweep (FBS) method [46], where the optimal solution is obtained using a forward-backward iterative method with a Runge-Kutta fourth-order solver. However, the convergence of the method depends on the initialisation of the control and on the choices of the parameters of the model [46]. Heuristic optimisation algorithms, such as the simulated annealing method, are employed when FBS fails to converge [151].

We conclude with some examples of the application of optimal control theory in epidemic control: [152] describes the dynamic optimal vaccination strategy for an SIR epidemic model and obtains the optimal solution using the FBS algorithm; [153] solves the optimal control problem of minimising the total level of infection when the control actions are bounded due to scarce resources; [55] discusses optimal vaccination strategies for horizontally and vertically transmitted infectious diseases; [154] leverages the Pontryagin maximum principle to determine an optimal Bang-Bang strategy that minimises the total number of infection cases during the spread of SIR epidemics in contact networks. An example of the optimal control of the present COVID-19 pandemic is proposed in [11], [155], where the authors

design an optimal strategy aimed at minimising the number of infected cases while reducing the cost of NPIs. Of particular relevance is model predictive control, which can ensure both optimality and robustness [57], [60] when contrasting outbreaks, in spite of possible model inaccuracy and strong parameter uncertainties.

C. Behavioural Modelling

Classical epidemiological models represent individuals as interacting particles following the empirical mass-action law (also employed in chemical reaction networks), resulting in a well-mixed population. However, people have specific contact patterns based on their habits and regular interactions; moreover, the individual behaviour during an epidemic is the result of a balance between usual habits and the information achieved on the epidemic evolution at a precise time. Also, the willingness to vaccinate results from a trade-off between the fear of contagion and the fear of vaccine-induced side effects: hence, the overall vaccine coverage is the outcome of individual decisions based on publicly available information on the current state of the disease and on possible side effects. Behavioural change models have been developed [63], [64], [66] to embed opinion-driven human actions as a key element that drives the spread of a disease.

The first work that explicitly includes a phenomenological behavioural response into the Kermack-McKendrick epidemic model is probably [84]. Further, the analysis of data regarding the spread of a cholera epidemic in Southern Italy in 1973 suggested the introduction of a nonlinear force of infection – in the term βSI, the linear I is replaced by a nonlinear function of I – that explains the emerging behaviour [156]. Typical expressions of nonlinear forces of infection are the so-called Holling type functional responses [84]

$$f(I) = \frac{\alpha I^p}{1 + \beta I^q}, \quad p, q > 0. \tag{29}$$

The cases $p = q = 1$ and $p = q = 2$ include saturation phenomena for large numbers of infected. Further, the choice $p = 1, q = 2$ models psychological effects: when the number of infected individuals is very large, the force of infection f decreases as I increases [84].

This concept is further elaborated in [157], which introduces a nonlinear dependence on the fraction of susceptible and infected individuals in AIDS models. [158] adds a delay in the force of infection.

The idea of a nonlinear force of infection motivated the development of the so-called behavioural epidemiology [61]–[66], which also studies the impact of human decisions on vaccine uptake under voluntary vaccination. When vaccination is voluntary, and not mandatory, records of disease control, due to a past vaccine-induced herd immunity, can favour the spread of information-dependent behaviour [65]. Moreover, in periods of low prevalence, individuals may encourage information and rumours on vaccine side-effects. As a result, their propensity to vaccinate might decline. On the contrary, during severe outbreaks the attitude to vaccinate can increase [151] due to the increased fear of being infected. In [63], individual decisions on vaccination are assumed to rely not only on the present situation, but also on past information about the spread of the disease, which is mathematically described by the information index

$$M(t) = \int_{-\infty}^{t} g(y(s))K(t-s)ds, \tag{30}$$

where K is the delaying kernel encoding the relevance of past information for the population and the function g, representing the information that individuals consider relevant when making their choices, depends on the variable y, which is the system state, e.g. $y = (S, I, R)^\top$ in a SIR model. The index M encodes information about the current and past states of the disease. It is a time-delayed formulation since information takes time to reach the population. Specifically, the kernel is assumed to belong to the Erlangian family: $K(t) = Erl_{n,a}(t) = \frac{a^n}{(n-1)!} t^{n-1} e^{-at}$, $a, t \in \mathbb{R}^+, n \in \mathbb{N}$.

Recent examples of the use of behavioural modelling of infectious diseases apply the information index to simple models containing distinctive relevant features of a coronavirus disease [61] and take into account vaccine hesitancy and refusal in the context of the COVID-19 pandemic, showing how information-related parameters affect the disease dynamics [62]. Large information coverage and small memory characteristic time are needed to have the best results in terms of vaccine coverage. Also, [151] applies optimal control on a behavioural model of the SIR type with voluntary vaccination and public health system interventions to determine the vaccination shape in childhood diseases.

D. Bridging Scales: Multi-Scale Epidemiological Models

The onset and the spread of infectious diseases are phenomena that inherently involve different scales, ranging from in-host infection dynamics at the patient level to between-host contagion dynamics at the population level. Therefore, the most complex, all-encompassing models of epidemic phenomena are multi-scale models [85]–[97], [100], [159]–[162], which capture both in-host and between-host dynamics with a nested approach [93], [159], [163] and study how the former affects the latter [90] by considering the interplay between the immunological mechanisms in the host and the epidemiological mechanisms of contagion.

The coupling between infection dynamics and contagion dynamics is due to the fact that the infectiousness of an individual host varies throughout the course of the infection, due to changes in pathogen loads and in the behavioural responses to infection [96], [98], [163], [164]. Multi-scale models use an in-host model, whose parameters are chosen based on patient data, to determine the parameters of a population-scale model with time-dependent infectiousness [100], [163], by leveraging an assumed relationship between the infection level within a host and the rate at which the host transmits the pathogen to susceptible individuals [96], [98], [100], [163]. Not only patient-level infection dynamics affect the population-scale transmission of contagion: a feedback from the population to the patient level may be present e.g. due to multiple co-circulating pathogen strains [96], [163].

Multi-scale epidemiological modelling studies are relatively numerous, but only few of them comprehensively use real data, partly because of the lack of suitable datasets and partly because of the huge complexity and challenging implementation of such models [96]–[98]. Streamlining these models and making them amenable to tackle real-time epidemics in combination with actual epidemiological data is fundamental so as to enable the design of coordinated control interventions that concurrently act both at the individual level and at the population level, thus bridging the inherent scales of an epidemic not only from an understanding standpoint, but also from a control perspective.

V. Conclusions and Future Directions

We have presented models and control approaches to contrast the onset and the spread of infectious diseases at all scales, ranging from in-host infection dynamics to between-host contagion dynamics described adopting both compartmental and networked models.

Open problems in the analysis of spread processes evolving over networks include global stability analysis of the endemic equilibrium for the discrete-time networked SIS and SIRS models, and a complete analysis of the stability of the endemic equilibria for the continuous time SAIRS networked and compartment models. Further, exploring the case of parameter estimation for networked epidemiological models in the presence of noise, with provable bounds, is an open problem. Efforts to explore the development of complete, closed-loop modelling and mitigation frameworks from testing data, through to control implementations have only recently been considered [165].

A broader overview including recently developed systems-and-control methodologies for present and future epidemics, with a strong emphasis on data-driven approaches and on issues related to monitoring and data collection, modelling, parameter estimation and identification, as well as control, is provided in [33] along with open problems. For a discussion of challenges and promising directions in epidemic control, the reader is referred to [130].

Here, we point out that a particularly fascinating direction for future interdisciplinary research is the development of holistic models that seamlessly integrate multiple resolution scales, from the immunological to the epidemiological level, include the effect of human behaviour and describe the multi-faceted impact of epidemics on healthcare along with socio-economical aspects, so as to develop all-encompassing control approaches that are coordinated across scales.

Acknowledgements

The authors wish to thank Teodoro Alamo for precious discussions and feedback.

References

[1] D. Bernoulli, "Essai d'une nouvelle analyse de la mortalité causée par la petite vérole et des avantages de l'inoculation pour la prévenir," *Histoire de l'Acad. Roy. Sci. avec Mém. des Math. et Phys. and Mém*, pp. 1–45, 1760.

[2] W. Kermack and A. McKendrick, "A contribution to the mathematical theory of epidemics," *Proc. Royal Society A*, vol. 115: 772, 1927.

[3] W. O. Kermack and A. G. McKendrick, "Contributions to the mathematical theory of epidemics. II. The problem of endemicity," *Proc. Royal Society A*, vol. 138, no. 834, pp. 55–83, 1932.

[4] R. M. Anderson and R. May, *Infectious diseases of humans: dynamics and control*. Oxford University Press, 1992.

[5] F. Brauer and C. Castillo-Chavez, "Mathematical models in population biology and epidemiology," *Springer*, vol. 2nd ed., 2012.

[6] D. Breda, O. Diekmann, W. F. de Graaf, A. Pugliese, and R. Vermiglio, "On the formulation of epidemic models (an appraisal of Kermack and McKendrick)," *Journal of Biological Dynamics*, vol. 6, pp. 103–117, 2012.

[7] O. Diekmann and J. A. P. Heesterbeek, "Mathematical epidemiology of infectious diseases: Model building, analysis and interpretation," *Wiley*, 2000.

[8] H. Hethcote, "The mathematics of infectious diseases," *SIAM Review*, vol. 42, no. 4, pp. 599–653, 2000.

[9] C. Rothe, *et al.*, "Transmission of 2019-nCoV infection from an asymptomatic contact in Germany," *New England Journal of Medicine*, vol. 382, p. 970–971, 2020.

[10] S. Mallapaty, "Antibody tests suggests coronavirus infections vastly exceed official counts," *Nature, News article*, 2020.

[11] M. Mandal, S. Jana, S. K. Nandi, A. Khatua, S. Adak, and T. Kar, "A model based study on the dynamics of COVID-19: Prediction and control," *Chaos, Solitons and Fractals*, vol. 136, 109889, 2020.

[12] L. Stella, A. P. Martínez, D. Bauso, and P. Colaneri, "The role of asymptomatic infections in the COVID-19 epidemic via complex networks and stability analysis," *SIAM J. Control Optimization*, 2022.

[13] X. Bi and C. Beck, "On the role of asymptomatic carriers in epidemic spread processes," *arXiv preprint arXiv:2103.11411*, 2021, shorter version in Proceedings, ACC 2021.

[14] A. B. Gumel, *et al.*, "Modelling strategies for controlling SARS outbreaks," *Proc. R. Soc. B Biol. Sci.*, vol. 271(1554), pp. 2223–32, 2004.

[15] G. Giordano, F. Blanchini, R. Bruno, P. Colaneri, A. Di Filippo, A. Di Matteo, and M. Colaneri, "Modelling the COVID-19 epidemic and implementation of population-wide interventions in Italy," *Nature Medicine*, vol. 26, pp. 855–860, 2020.

[16] G. Giordano, M. Colaneri, A. Di Filippo, F. Blanchini, P. Bolzern, G. De Nicolao, P. Sacchi, P. Colaneri, and R. Bruno, "Modeling vaccination rollouts, SARS-CoV-2 variants and the requirement for non-pharmaceutical interventions in Italy," *Nature Medicine*, 2021.

[17] W. Mei, S. Mohagheghi, S. Zampieri, and F. Bullo, "On the dynamics of deterministic epidemic propagation over networks," *Annual Reviews in Control*, vol. 44, pp. 116 – 128, 2017.

[18] C. Nowzari, V. M. Preciado, and G. J. Pappas, "Analysis and control of epidemics: A survey of spreading processes on complex networks," *IEEE Control Systems Magazine*, no. 1, pp. 26–46, 2016.

[19] P. Pare, C. L. Beck, and T. Basar, "Modeling, estimation and analysis of epidemics over networks: an overview," *Annual Reviews in Control*, pp. 345–360, 2020.

[20] R. Pastor-Satorras, C. Castellano, P. Van Mieghem, and A. Vespignani, "Epidemic processes in complex networks," *Reviews of Modern Physics*, vol. 87, no. 3, p. 925, 2015.

[21] L. Canini and A. S. Perelson, "Viral kinetic modeling: state of the art," *Journal of Pharmacokinetics and Pharmacodynamics*, vol. 41, pp. 431–443, 2014.

[22] F. Castiglione and F. Celada, *Immune System Modelling and Simulation*. CRC Press, Boca Raton, 2015.

[23] A. Handel, I. M. Longini, and R. Antia, "Towards a quantitative understanding of the within-host dynamics of influenza A infections," *Journal of the Royal Society Interface*, vol. 7, no. 42, pp. 35–47, 2010.

[24] K. Li, J. M. McCaw, and P. Cao, "Modelling within-host macrophage dynamics in influenza virus infection," *Journal of Theoretical Biology*, vol. 508, p. 110492, 2021.

[25] A. S. Perelson, "Modelling viral and immune system dynamics," *Nature Reviews Immunology*, vol. 2, pp. 28–36, 2002.

[26] A. W. Yan, P. Cao, J. M. Heffernan, J. McVernon, K. M. Quinn, N. L. La Gruta, K. L. Laurie, and J. M. McCaw, "Modelling cross-reactivity and memory in the cellular adaptive immune response to influenza infection in the host," *Journal of Theoretical Biology*, vol. 413, pp. 34–49, 2017.

[27] E. Hernandez-Vargas, P. Colaneri, R. Middleton, and F. Blanchini, "Discrete-time control for switched positive systems with application

to mitigating viral escape," *International Journal of Robust and Nonlinear Control*, vol. 21, no. 10, pp. 1093–1111, 2011.

[28] P. Colaneri, R. H. Middleton, Z. Chen, D. Caporale, and F. Blanchini, "Convexity of the cost functional in an optimal control problem for a class of positive switched systems," *Automatica*, vol. 50, no. 4, pp. 1227–1234, 2014.

[29] E. A. Hernandez-Vargas, P. Colaneri, and R. H. Middleton, "Switching strategies to mitigate HIV mutation," *IEEE Transactions on Control Systems Technology*, vol. 22, no. 4, pp. 1623–1628, 2014.

[30] G. Giordano, A. Rantzer, and V. D. Jonsson, "A convex optimization approach to cancer treatment to address tumor heterogeneity and imperfect drug penetration in physiological compartments," in *2016 IEEE 55th Conference on Decision and Control (CDC)*, 2016, pp. 2494–2500.

[31] C. A. Devia and G. Giordano, "Optimal duration and planning of switching treatments taking drug toxicity into account: a convex optimisation approach," in *2019 IEEE 58th Conference on Decision and Control (CDC)*, 2019, pp. 5674–5679.

[32] N. Dullerud and V. D. Jonsson, "Cellular immunotherapy treatment scheduling to address antigen escape," in *2020 59th IEEE Conference on Decision and Control (CDC)*, 2020, pp. 4634–4639.

[33] T. Alamo, D. G. Reina, P. M. Gata, V. M. Preciado, and G. Giordano, "Data-driven methods for present and future pandemics: Monitoring, modelling and managing," *Annual Reviews in Control*, vol. 52, pp. 448–464, 2021.

[34] M. T. Angulo, F. Castaños, R. Moreno-Morton, J. X. Velasco-Hernández, and J. A. Moreno, "A simple criterion to design optimal non-pharmaceutical interventions for mitigating epidemic outbreaks," *Journal of The Royal Society Interface*, vol. 18, no. 178, p. 20200803, 2021.

[35] F. Avram, L. Freddi, and D. Goreac, "Optimal control of a SIR epidemic with ICU constraints and target objectives," *Applied Mathematics and Computation*, vol. 418, p. 126816, 2022.

[36] H. Behncke, "Optimal control of deterministic epidemics," *Optimal Control Applications and Methods*, vol. 21, no. 6, pp. 269–285, 2000.

[37] P.-A. Bliman, M. Duprez, Y. Privat, and N. Vauchelet, "Optimal immunity control and final size minimization by social distancing for the SIR epidemic model," *Journal of Optimization Theory and Applications*, vol. 189, pp. 408–436, 2021.

[38] M. Bloem, T. Alpcan, and T. Basar, "Optimal and robust epidemic response for multiple networks," *Control Engineering Practice*, vol. 17, pp. 525–533, 2009.

[39] L. Bolzoni, E. Bonacini, C. Soresina, and M. Groppi, "Time-optimal control strategies in SIR epidemic models," *Mathematical Biosciences*, vol. 292, pp. 86–96, 2017.

[40] L. Bolzoni, E. Bonacini, R. Della Marca, and M. Groppi, "Optimal control of epidemic size and duration with limited resources," *Mathematical Biosciences*, vol. 315, p. 108232, 2019.

[41] L. Freddi, "Optimal control of the transmission rate in compartmental epidemics," *Mathematical Control and Related Fields*, vol. 12, no. 1, pp. 201–223, 2022.

[42] H. Gaff and E. Schaefer, "Optimal control applied to vaccination and treatment strategy for various epidemiological models," *Math Biosci Eng MBE*, vol. 6(3), pp. 469–492, 2009.

[43] E. Hansen and T. Day, "Optimal control of epidemics with limited resources," *Journal of Mathematical Biology*, vol. 62, pp. 423–451, 2011.

[44] M. Kantner and T. Koprucki, "Beyond just "flattening the curve": Optimal control of epidemics with purely non-pharmaceutical interventions," *Journal of Mathematics in Industry*, vol. 10, p. 23, 2020.

[45] D. I. Ketcheson, "Optimal control of an SIR epidemic through finite-time non-pharmaceutical intervention," *Journal of Mathematical Biology*, vol. 83, p. 7, 2021.

[46] S. Lenhart and J. T. Workman, "Optimal control applied to biological models," *Chapman and Hall, CRC*, 2007.

[47] M. Martcheva, "An introduction to mathematical epidemiology," *Springer Science and Business Media LLC*, 2015.

[48] D. H. Morris, F. W. Rossine, J. B. Plotkin, and S. A. Levin, "Optimal, near-optimal, and robust epidemic control," *Communications Physics*, vol. 4, p. 78, 2021.

[49] R. Morton and K. H. Wickwire, "On the optimal control of a deterministic epidemic," *Advances in Applied Probability*, vol. 6, pp. 622–635, 1974.

[50] O. Sharomi and T. Malik, "Optimal control in epidemiology," *Annals of Operations Research*, vol. 251, pp. 55–71, 2017.

[51] E. H. Bussell, C. E. Dangerfield, C. A. Gilligan, and N. J. Cunniffe, "Applying optimal control theory to complex epidemiological models to inform real-world disease management," *Philosophical Transactions of the Royal Society B: Biological Sciences*, vol. 374, no. 1776, p. 20180284, 2019.

[52] V. Priesemann, *et al.*, "Calling for pan-European commitment for rapid and sustained reduction in SARS-CoV-2 infections," *The Lancet*, vol. 397, no. 10269, pp. 92–93, 2021.

[53] ——, "An action plan for pan-European defence against new SARS-CoV-2 variants," *The Lancet*, vol. 397, no. 10273, pp. 469–470, 2021.

[54] E. Asano, L. Gross, S. Lenhart, and L. Real, "Optimal control of vaccine distribution in a rabies metapopulation model," *Math. Biosci. Eng.*, vol. 5, pp. 219–238, 2008.

[55] B. Buonomo, "On the optimal vaccination strategies for horizontally and vertically transmitted infectious diseases," *Journal of Biological Systems*, vol. 19, pp. 263–279, 2011.

[56] M. Bin, *et al.*, "Post-lockdown abatement of COVID-19 by fast periodic switching," *PLOS Computational Biology*, vol. 17, no. 1, pp. 1–34, 2021.

[57] J. Köhler, L. Schwenkel, A. Koch, J. Berberich, P. Pauli, and F. Allgöwer, "Robust and optimal predictive control of the COVID-19 outbreak," *Annual Reviews in Control*, vol. 51, pp. 525–539, 2021.

[58] T. Krueger, *et al.*, "Risk assessment of COVID-19 epidemic resurgence in relation to SARS-CoV-2 variants and vaccination passes," *Communications Medicine*, vol. 2, 2022.

[59] G. Leitmann, "The use of screening for the control of an endemic disease," *Variational Calculus, Optimal Control and Applications*, vol. 124, pp. 291—300, 1998.

[60] M. M. Morato, S. B. Bastos, D. O. Cajueiro, and J. E. Normey-Rico, "An optimal predictive control strategy for COVID-19 (SARS-CoV-2) social distancing policies in Brazil," *Annual Reviews in Control*, vol. 50, pp. 417–431, 2020.

[61] B. Buonomo, "Effects of information-dependent vaccination behavior on coronavirus outbreak: insights from a SIRI model," *Ricerche mat*, vol. 69, p. 483–499, 2020.

[62] B. Buonomo, R. Della Marca, A. d'Onofrio, and M. Groppi, "A behavioural modelling approach to assess the impact of COVID-19 vaccine hesitancy," *Journal of Theoretical Biology*, vol. 534, p. 110973, 2022.

[63] A. d'Onofrio, P. Manfredi, and E. Salinelli, "Vaccinating behaviour, information, and the dynamics of SIR vaccine preventable diseases." *Theor Popul Biol*, vol. 71, pp. 301–317, 2007.

[64] S. Funk, M. Salathé, and V. Jansen, "Modelling the influence of human behaviour on the spread of infectious diseases: a review," *J R Soc Interface*, vol. 7, pp. 1247–1256, 2010.

[65] P. Manfredi and A. d'Onofrio, "Modeling the interplay between human behavior and the spread of infectious diseases," *Springer, New York*, 2013.

[66] Z. Wang, C. Bauch, S. Bhattacharyya, A. d'Onofrio, P. Manfredi, M. Perc, N. Perra, M. Salathé, and D. Zhao, "Statistical physics of vaccination." *Phys Rep*, vol. 664, pp. 1–113, 2016.

[67] M. Draief and L. Massoulie', *Epidemics and rumours in complex networks*. Cambridge University Press, 2010.

[68] P. Van Mieghem, J. Omic, and R. Kooij, "Virus spread in networks," *IEEE/ACM Transactions on Networking*, no. 1, pp. 62–68, 2009.

[69] S. Chatterjee and R. Durrett, "Contact processes on random graphs with power law degree distributions have critical value 0," *The Annals of Probability*, no. 6, pp. 2332–2356, 2009.

[70] A. Fall, A. Iggidr, G. Sallet, and J. J. Tewa, "Epidemiological models and Lyapunov functions," *Mathematical Modelling of Natural Phenomena*, vol. 2, no. 1, pp. 62–83, 2007.

[71] P. E. Paré, C. L. Beck, and A. Nedić, "Epidemic processes over time-varying networks," *IEEE Transactions on Control over Network Systems*, no. 3, pp. 1322–1334, 2018.

[72] Y. Wang, D. Chakrabarti, C. Wang, and C. Faloutsos, "Epidemic spreading in real networks: an eigenvalue viewpoint," in *Proc. 22nd Intern. Symp. Reliable Distributed Systems*, 2003, pp. 25–34.

[73] H. J. Ahn and B. Hassibi, "Global dynamics of epidemic spread over complex networks," in *Proc. IEEE Conference on Decision and Control*, 2013, pp. 4579–4585.

[74] P. E. Paré, J. Liu, C. L. Beck, B. E. Kirwan, and T. Başar, "Analysis, identification, and validation of discrete-time epidemic processes," *IEEE Transactions on Control Systems Technology*, vol. 28, no. 1, pp. 79–93, 2019.

[75] A. Khanafer, T. Başar, and B. Gharesifard, "Stability properties of infected networks with low curing rates," in *Proc. American Control Conference*, 2014, pp. 3579–3584.

[76] ——, "Stability properties of infection diffusion dynamics over directed networks," in *Proc. IEEE Conference on Decision and Control*, 2014, pp. 6215–6220.

[77] C. Nowzari, V. M. Preciado, and G. J. Pappas, "Stability analysis of generalized epidemic models over directed networks," in *Proc. IEEE Conference on Decision and Control*, 2014, pp. 6197–6202.

[78] J. Liu, P. E. Paré, A. Nedić, C. Y. Tang, C. L. Beck, and T. Başar, "Analysis and control of a continuous-time bi-virus model," *IEEE Transactions on Automatic Control*, vol. 64, no. 12, pp. 4891–4906, 2019.

[79] P. Van Mieghem, "Exact Markovian SIR and SIS epidemics on networks and an upper bound for the epidemic threshold," *arXiv preprint arXiv:1402.1731*, 2014.

[80] J. L. Gevertz, J. M. Greene, C. H. Sanchez-Tapia, and E. D. Sontag, "A novel COVID-19 epidemiological model with explicit susceptible and asymptomatic isolation compartments reveals unexpected consequences of timing social distancing," *Journal of Theoretical Biology*, vol. 510, p. 110539, 2021.

[81] G. De Nicolao, G. Giordano, M. Colaneri, A. D. Filippo, F. Blanchini, P. Bolzern, P. Colaneri, P. Sacchi, and R. Bruno, "The toll of procrastination in epidemic control: a pre-emptive periodic strategy saves lives without increasing socio-economic costs," in *29th Mediterranean Conference on Control and Automation (MED)*, 2021.

[82] E. D. Sontag, "An explicit formula for minimizing the infected peak in an SIR epidemic model when using a fixed number of complete lockdowns," *International Journal of Robust and Nonlinear Control*, 2021.

[83] S. Sturniolo, W. Waites, T. Colbourn, D. Manheim, and J. Panovska-Griffiths, "Testing, tracing and isolation in compartmental models," *PLOS Computational Biology*, vol. 17, no. 3, pp. 1–28, 2021.

[84] V. Capasso and G. Serio, "A generalization of kermack-mckendrick deterministic epidemic model," *Mathematical Biosciences*, vol. 42, pp. 43–61, 1978.

[85] N. Bellomo, R. Bingham, M. A. J. Chaplain, G. Dosi, G. Forni, D. A. Knopoff, J. Lowengrub, R. Twarock, and M. E. Virgillito, "A multiscale model of virus pandemic: Heterogeneous interactive entities in a globally connected world," *Mathematical Models and Methods in Applied Sciences*, vol. 30, no. 08, pp. 1591–1651, 2020.

[86] S. Alizon, F. Luciani, and R. R. Regoes, "Epidemiological and clinical consequences of within-host evolution," *Trends in Microbiology*, vol. 19, pp. 24–32, 2011.

[87] A. E. S. Almocera, V. K. Nguyen, and E. A. Hernandez-Vargas, "Multiscale model within-host and between-host for viral infectious diseases," *Journal of Mathematical Biology*, vol. 77, pp. 1035–1057, 2018.

[88] A. E. S. Almocera and E. A. Hernandez-Vargas, "Coupling multiscale within-host dynamics and between-host transmission with recovery (SIR) dynamics," *Mathematical Biosciences*, vol. 309, pp. 34–41, 2019.

[89] M. Barbarossa and G. Röst, "Immuno-epidemiology of a population structured by immune status: a mathematical study of waning immunity and immune system boosting," *Journal of Mathematical Biology*, vol. 71, pp. 1737–1770, 2015.

[90] L. Cai, N. Tuncer, and M. Martcheva, "How does within-host dynamics affect population-level dynamics? insights from an immuno-epidemiological model of malaria," *Mathematical Methods in the Applied Sciences*, vol. 40, no. 18, pp. 6424–6450, 2017.

[91] Z. Feng, J. Velasco-Hernandez, B. Tapia-Santos, and M. Leite, "A model for coupling within-host and between-host dynamics in an infectious disease," *Nonlinear Dynamics*, vol. 68, pp. 401–411, 2012.

[92] Z. Feng, X. Cen, Y. Zhao, and J. X. Velasco-Hernandez, "Coupled within-host and between-host dynamics and evolution of virulence," *Mathematical Biosciences*, vol. 270, pp. 204–212, 2015, from Within-Host Dynamics to the Epidemiology of Infectious Disease.

[93] A. Gandolfi, A. Pugliese, and C. Sinisgalli, "Epidemic dynamics and host immune response: a nested approach," *Journal of Mathematical Biology*, vol. 70, pp. 399–435, 2015.

[94] R. B. Garabed, A. Jolles, W. Garira, C. Lanzas, J. Gutierrez, and G. Rempala, "Multi-scale dynamics of infectious diseases," *Interface Focus*, vol. 10, p. 1020190118, 2020.

[95] W. Garira, "A primer on multiscale modelling of infectious disease systems," *Infectious Disease Modelling*, vol. 3, pp. 176–191, 2018.

[96] W. S. Hart, P. K. Maini, C. A. Yates, and R. N. Thompson, "A theoretical framework for transitioning from patient-level to population-scale epidemiological dynamics: influenza A as a case study," *Journal of the Royal Society Interface*, vol. 17, p. 20200230, 2020.

[97] L. M. Childs, F. El Moustaid, Z. Gajewski, S. Kadelka, R. Nikin-Beers, J. W. Smith Jr, M. Walker, and L. R. Johnson, "Linked within-host and between-host models and data for infectious diseases: a systematic review," *PeerJ*, vol. 7, p. e7057, 2019.

[98] A. Handel and P. Rohani, "Crossing the scale from within-host infection dynamics to between-host transmission fitness: a discussion of current assumptions and knowledge," *Philosophical Transactions of the Royal Society B: Biological Sciences*, vol. 370, no. 1675, p. 20140302, 2015.

[99] E. A. Hernandez-Vargas, A. Y. Alanis, and J. Tetteh, "A new view of multiscale stochastic impulsive systems for modeling and control of epidemics," *Annual Reviews in Control*, vol. 48, pp. 242–249, 2019.

[100] L. N. Murillo, M. S. Murillo, and A. S. Perelson, "Towards multiscale modeling of influenza infection," *Journal of Theoretical Biology*, vol. 332, pp. 267–290, 2013.

[101] E. A. Hernandez-Vargas, *Feedback control for personalized medicine*, 1st ed. ELSEVIER Academic Press, 2022.

[102] K. Murphy and C. Weaver, *Janeway's Immunobiology*, 8th ed. Garland Science, 2016.

[103] C. Parra-Rojas and E. A. Hernandez-Vargas, "PDEparams: parameter fitting toolbox for partial differential equations in python," *Bioinformatics*, dec 2019.

[104] A. Raue, C. Kreutz, T. Maiwald, J. Bachmann, M. Schilling, U. Klingmuller, and J. Timmer, "Structural and practical identifiability analysis of partially observed dynamical models by exploiting the profile likelihood," *Bioinformatics*, vol. 25, pp. 1923–1929, 2009.

[105] B. Efron and R. Tibshirani, "[bootstrap methods for standard errors, confidence intervals, and other measures of statistical accuracy]: Rejoinder," *Statistical Science*, vol. 1, pp. 54–75, 1986.

[106] M. M. Morato, I. M. L. Pataro, M. V. Americano da Costa, and J. E. Normey-Rico, "A parametrized nonlinear predictive control strategy for relaxing covid-19 social distancing measures in brazil," *ISA Transactions*, vol. 124, pp. 197–214, 2022.

[107] H. Akaike, "A new look at the statistical model identification," *IEEE Transactions on Automatic Control*, vol. 19, no. 6, pp. 716–723, 1974.

[108] S. M. Ciupe and J. M. Heffernan, "In-host modeling," *Infectious Disease Modelling*, vol. 2, pp. 188–202, 2017.

[109] E. Kirschner and F. Webb, "Immunotherapy of HIV-1 infection," *Journal of Biological Systems*, vol. 6, p. 71–83, 1998.

[110] A. S. Perelson and J. Guedj, "Modelling hepatitis C therapy: predicting effects of treatment." *Nature reviews. Gastroenterology and hepatology*, vol. 12, pp. 437–45, 8 2015.

[111] K. A. Pawelek, D. Dor, C. Salmeron, and A. Handel, "Within-host models of high and low pathogenic influenza virus infections: The role of macrophages," *PLoS ONE*, vol. 11, pp. 1–16, 2016.

[112] V. K. Nguyen and E. A. Hernandez-Vargas, "Windows of opportunity for Ebola virus infection treatment and vaccination." *Scientific reports*, vol. 7, p. 8975, 2017.

[113] C. E. Osuna, *et al.*, "Zika viral dynamics and shedding in rhesus and cynomolgus macaques," *Nature medicine*, vol. 22, pp. 1448–1455, 2016.

[114] E. A. Hernandez-Vargas and J. X. Velasco-Hernandez, "In-host mathematical modelling of COVID-19 in humans," *Annual Reviews in Control*, 2020.

[115] M. Pérez, P. Abuin, M. Actis, A. Ferramosca, E. A. Hernandez-Vargas, and A. H. González, "Optimal control strategies to tailor antivirals for acute infectious diseases in the host: a study case of COVID-19," in *Feedback Control for Personalized Medicine*. Elsevier Academic Press, 2022, pp. 11–39.

[116] E. A. Hernandez-Vargas, *Modeling and Control of Infectious Diseases: with MATLAB and R*, 1st ed. ELSEVIER Academic Press, 2019.

[117] P. Abuin, A. Anderson, A. Ferramosca, E. A. Hernandez-Vargas, and A. H. Gonzalez, "Dynamical characterization of antiviral effects in COVID-19," *Annual reviews in control*, vol. 52, pp. 587–601, 2021.

[118] J. Sereno, A. D'Jorge, A. Ferramosca, E. Hernandez-Vargas, and A. González, "Model predictive control for optimal social distancing in a type SIR-switched model," *Ifac-papersonline*, vol. 54, no. 15, pp. 251–256, 2021.

[119] R. Ke, C. Zitzmann, D. D. Ho, R. M. Ribeiro, and A. S. Perelson, "In vivo kinetics of SARS-CoV-2 infection and its relationship with

a person's infectiousness," *Proc. National Academy of Sciences*, vol. 118, no. 49, 2021.

[120] P. van den Driessche and J. Watmough, "Reproduction numbers and sub-threshold endemic equilibria for compartmental models of disease transmission," *Mathematical Biosciences*, vol. 180, no. 1, pp. 29–48, 2002.

[121] M. Grunnill, "An exploration of the role of asymptomatic infections in the epidemiology of dengue viruses through susceptible, asymptomatic, infected and recovered (SAIR) models," *Journal of Theoretical Biology*, vol. 439, pp. 195–204, 2018.

[122] H. K. Khalil, *Nonlinear Systems*. Prentice Hall, 2002.

[123] A. Khanafer, T. Başar, and B. Gharesifard, "Stability of epidemic models over directed graphs: a positive systems approach," *Automatica*, vol. 74, pp. 126–134, 2016.

[124] P. Van Mieghem and J. Omic, "In-homogeneous virus spread in networks," *arXiv preprint arXiv:1306.2588v2*, 2014.

[125] A. Lajmanovich and J. A. Yorke, "A deterministic model for gonorrhea in a nonhomogeneous population," *Mathematical Biosciences*, vol. 28, no. 3-4, pp. 221–236, 1976.

[126] F. Liu, S. Cui, X. Li, and M. Buss, "On the stability of the endemic equilibrium of a discrete-time networked epidemic model," in *Proc. IFAC World Congress*, 2020, pp. 1–6.

[127] P. E. Paré, J. Liu, C. L. Beck, A. Nedić, and T. Başar, "Multi-competitive viruses over time–varying networks with mutations and human awareness," *Automatica*, 2021.

[128] R. Pagliara and N. E. Leonard, "Adaptive susceptibility and heterogeneity in contagion models on networks," *IEEE Transactions on Automatic Control*, pp. 1–1, 2020.

[129] P. E. Paré, J. Liu, C. L. Beck, and T. Başar, "Networked infectious disease–contaminated water model," in *Proc. 18th European Control Conference (ECC)*, 2019, pp. 2018–2023.

[130] T. Alamo, P. Millán, D. G. Reina, V. M. Preciado, and G. Giordano, "Challenges and future directions in pandemic control," *IEEE Control Systems Letters*, vol. 6, pp. 722–727, 2022.

[131] G. Chowell, P. Fenimore, M. Castillo-Garsow, and C. Castillo-Chavez, "SARS outbreaks in Ontario, Hong Kong and Singapore: the role of diagnosis and isolation as a control mechanism," *Journal of Theoretical Biology*, vol. 224, pp. 1–8, 2003.

[132] S. Maharaj and A. Kleckowski, "Controlling epidemic spread by social distancing: do it well or not at all," *BMC Public Health*, vol. 12, p. 679, 2012.

[133] G. Calafiore, C. Novara, and C. Possieri, "A time-varying SIRD model for the COVID-19 contagion in Italy," *Annual Reviews in Control*, vol. 50, pp. 361–372, 2020.

[134] A. Cori, N. Ferguson, C. Fraser, and S. Cauchemez, "A new framework and software to estimate time-varying reproduction numbers during epidemics," *American Journal of Epidemiology*, vol. 178, pp. 1505–1512, 2013.

[135] Y. Fang, Y. Nie, and M. Penny, "Transmission dynamics of the COVID-19 outbreak and effectiveness of government intervention: a data-driven analysis," *Journal of Medical Virology*, pp. 1–15, 2020.

[136] F. Ball, T. Britton, T. House, V. Isham, D. Mollison, L. Pellis, and G. Scalia Tomba, "Seven challenges for metapopulation models of epidemics, including households models," *Epidemics*, vol. 10, pp. 63–67, 2015.

[137] E. Bertuzzo, L. Mari, D. Pasetto, S. Miccoli, R. Casagrandi, M. Gatto, and A. Rinaldo, "The geography of COVID-19 spread in Italy and implications for the relaxation of confinement measures," *Nature Communications*, vol. 11, p. 4264, 2020.

[138] F. Della Rossa, *et al.*, "A network model of Italy shows that intermittent regional strategies can alleviate the COVID-19 epidemic," *Nature Communications*, vol. 11, p. 5106, 2020.

[139] M. Gatto, E. Bertuzzo, L. Mari, S. Miccoli, L. Carraro, R. Casagrandi, and A. Rinaldo, "Spread and dynamics of the COVID-19 epidemic in Italy: Effects of emergency containment measures," *Proc. National Academy of Sciences*, vol. 117, no. 19, pp. 10 484–10 491, 2020.

[140] B. Grenfell and J. Harwood, "(Meta)population dynamics of infectious diseases," *Trends in Ecology & Evolution*, vol. 12, no. 10, pp. 395–399, 1997.

[141] S. Thurner, P. Klimek, and R. Hanel, "A network-based explanation of why most COVID-19 infection curves are linear," *Proc. National Academy of Sciences*, vol. 117, pp. 22 684–22 689, 2020.

[142] K. O. Kwok, A. Tang, V. W. Wei, W. H. Park, E. K. Yeoh, and S. Riley, "Epidemic models of contact tracing: Systematic review of transmission studies of severe acute respiratory syndrome and middle east respiratory syndrome," *Computational and Structural Biotechnology Journal*, vol. 17, pp. 186–194, 2019.

[143] N. Becker, "On a general stochastic epidemic model," *Theoretical Population Biology*, vol. 11, pp. 23–36, 1977.

[144] B. Graham, "Rapid COVID-19 vaccine development," *Science*, vol. 368, pp. 945–946, 2020.

[145] K. Hattaf, M. Rachik, S. Saadi, Y. Tabit, and N. Yousfi, "Optimal control of tuberculosis with exogenous reinfection," *Appl. Math. Sci.*, vol. 3, pp. 231–240, 2009.

[146] L. Cesari, "Existence theorems for optimal solutions in Pontryagin and Lagrange problems," *Journal of the Society for Industrial and Applied Mathematics Series A: Control*, vol. 3, pp. 475–498, 1965.

[147] A. Filippov, "On certain questions in the theory of optimal control," *Journal of Society for Industrial and Applied Mathematics Series A: Control*, vol. 1, pp. 76–84, 1962.

[148] L. S. Pontryagin, "On the theory of differential games," *Russian Mathematical Surveys*, vol. 21, no. 4, pp. 193–246, 1966.

[149] M. Kamien and N. Schwartz, "Sufficient conditions in optimal control theory," *Journal of Economic Theory*, vol. 3, pp. 207–214, 1971.

[150] A. Borzì, *Modelling with Ordinary Differential Equations: A Comprehensive Approach*, ser. Numerical Analysis and Scientific Computing Series. Chapman & Hall/CRC, Abingdon and Boca Raton, 2020.

[151] B. Buonomo, P. Manfredi, and A. d'Onofrio, "Optimal time-profiles of public health intervention to shape voluntary vaccination for childhood diseases," *J. Math. Biol.*, vol. 78, p. 1089–1113, 2019.

[152] G. Zaman, Y. Kang, and H. Jung, "Stability analysis and optimal vaccination of an SIR epidemic model," *BioSystems*, vol. 93, pp. 240–249, 2008.

[153] R. Rowthorn, R. Laxminarayan, and C. Gilligan, "Optimal control of epidemics in metapopulations," *Journal of the Royal Society Interface*, vol. 6, pp. 1135–1144, 2009.

[154] M. Youssef and C. Scoglio, "Mitigation of epidemics in contact networks through optimal contact adaptation," *Mathematical Biosciences and Engineering*, vol. 10, pp. 1227–1251, 2013.

[155] M. Hayhoe, F. Barreras, and V. Preciado, "Data-driven control of the COVID-19 outbreak via non-pharmaceutical interventions: A geometric programming approach," *arXiv 2011.01392*, 2020.

[156] V. Capasso and S. Paveri-Fontana, "Mathematical model for the 1973 cholera epidemic in the european mediterranean region," *Revue d'Epidémiologie et de Santé Publique*, vol. 27, pp. 121–132, 1979, errata corrige 28 (1980), 390.

[157] C. Castillo-Chavez, K. Cooke, W. Huang, and S. Levin, "On the role of long incubation periods in the dynamics of acquired immunodeficiency syndrome (aids) i. single population models," *Journal of Mathematical Biology*, vol. 27, pp. 373–398, 1989.

[158] E. Beretta and Y. Takeuchi, "Global stability of an SIR epidemic model with time delays," *Journal of Mathematical Biology*, vol. 33, pp. 250–260, 1995.

[159] T. Day, S. Alizon, and N. Mideo, "Bridging scales in the evolution of infectious disease life histories: Theory," *Evolution*, vol. 65, no. 12, pp. 3448–3461, 2011.

[160] M. A. Gilchrist and D. Coombs, "Evolution of virulence: Interdependence, constraints, and selection using nested models," *Theoretical Population Biology*, vol. 69, no. 2, pp. 145–153, 2006.

[161] A. Handel, J. Brown, D. Stallknecht, and P. Rohani, "A multi-scale analysis of influenza A virus fitness trade-offs due to temperature-dependent virus persistence," *PLOS Computational Biology*, vol. 9, no. 3, pp. 1–13, 2013.

[162] M. Legros and S. Bonhoeffer, "A combined within-host and between-hosts modelling framework for the evolution of resistance to anti-malarial drugs," *Journal of The Royal Society Interface*, vol. 13, no. 117, p. 20160148, 2016.

[163] N. Mideo, S. Alizon, and T. Day, "Linking within- and between-host dynamics in the evolutionary epidemiology of infectious diseases," *Trends in Ecology and Evolution*, vol. 23, pp. 511–517, 2008.

[164] W. Hart, L. Hochfilzer, N. Cunniffe, H. Lee, H. Nishiura, and R. Thompson, "Accurate forecasts of the effectiveness of interventions against ebola may require models that account for variations in symptoms during infection," *Epidemics*, vol. 29, p. 100371, 2019.

[165] A. R. Hota, J. Godbole, P. Bhariya, and P. E. Paré, "A closed-loop framework for inference, prediction and control of SIR epidemics on networks," 2020, https://arxiv.org/abs/2006.16185.